CTH-IEFT/PP-1990-03 ISSN

PRESTUDY OF BURN CONTROL IN NET

Second Intermediate Report, February 1990

D. Anderson, T. Elevant, H. Hamnén, M. Lisak, J. Lorenzen, H. Persson

INSTITUTIONEN FÖR ELEKTROMAGNETISK FÄLTTEORI

CHALMERS TEKNISKA HÖGSKOLA

CTH-IEFT/PP-1990-03

PRESTUDY OF BURN CONTROL IN NET

Second Intermediate Report, February 1990

By

D. Anderson, T. Elevant[1], H. Hamnén, M. Lisak, J. Lorenzen[2], H. Persson[2]

Chalmers University of Technology
Institute for Electromagnetic Field Theory and Plasma Physics
S-412 96 Göteborg, Sweden

[1]The Royal Institute for Technology
Plasma Physics and Fusion Research
S-100 44 Stockholm, Sweden

[2]Studsvik Nuclear
S-611 82 Nyköping, Sweden

Contents

1. Introduction

In the first intermediate report [1] we collected information on burn control in general, including a survey of control methods, and of the properties and limitations of various plasma diagnostics to be used in this connection. A direction for our work was given - among things emphasized were the importance of studying profile effects, the impact of diagnostics, and the need for a closer contact between plasma physics and control.

Since then, several interesting papers on burn control have appeared, including such with particular application to ITER [2,3].

The present report describes our ongoing work on a number of selected topics, and the plans for the nearest future.

In a zerodimensional model the key entity to linear stability of a working point and the nature of the trajectories near it is the matrix of the derivatives of the right-hand members with respect to the dependent variables, evaluated at the working point. Notably, stability prevails if the real parts of all eigenvalues of this matrix are negative.

In chapter 2 we have specialized the system (1) - (2) of the previous report to form an easily tractable, second-order system. In this case one can give an explicit, analytical condition for stability: the point is stable when the matrix has a negative trace and a positive determinant. A code providing quick answers regarding stability, time scales and eigenvectors has been written and tested.

To illustrate the properties of the multitude of solutions in a finite region, there hardly exists any better method than a qualitative phase-plane analysis, based upon equilibrium point classification, determination of various manifolds (fast, slow, stable, unstable), together with a suitably dense set of trajectories. We have implemented our system of equations

on an efficient ODE solver, providing such information. Time functions of various quantities can also be obtained. Feedback control of unstable working points has been tested in a number of cases. It is found that linear stability can often be obtained by simple means. However, nonlinear effects are sometimes quite important.

The zerodimensional modelling of a burning plasma described by space dependent equations is often done in a heuristic way, with no clear relation between the two systems of equations. We have tried to put the approximation procedure involved in the transition to 0-D models on a more formal basis. This is the topic of chapter 3. Simple and useful approximations of the radial equilibrium temperature profiles are derived for a class of nonlinear transport and heating models. The 1-D equilibrium solution is also investigated with respect to its stability properties, which are shown to be the same as those derived from the simplest 0-D space averaged model.

Chapter 4 contains a few emerging thoughts on burn control. First, the limited swing of the auxiliary heating gives rise to limitations on the possibilities to intervene against temperature excursions by an auxiliary heating modulation. This problem becomes severe when one operates at high Q values. Even a moderate temperature error, which one may well have due to the limited accuracy of the temperature measurements, may then lead to temperature runaway because there is perhaps not sufficiently much additional heating to reduce. This problem has been analysed in detail by Bromberg et al [4], it leads to a maximum allowable Q for given working temperature T_o and given temperature perturbation δT. We have found that the essential features of the results of these authors can be understood qualitatively, without much involved analysis.

Another analysis concerns the problem of selecting a proper control action when a temperature profile differs from the equilibrium shape.

Clearly, the change in axial temperature only is not sufficient to consider, but instead some sort of integral criterion is needed. One finds that thermal runaway is determined roughly by whether or not the instantaneous thermal energy content is more or less than that of the equilibrium. This is analysed in some detail, and a reasonably good criterion for thermal runaway is obtained.

The presence of sawteeth complicates active feedback control of an unstable equilibrium profile. Two aspects of this problem are tentatively discussed: (i) the profile change involved complicates interpretation of neutron emission signals and (ii) the sawtooth temperature variation implies an inherent Q-limitation for subignited situations. Distinguishing between the sawtooth excursions and real thermal runaway may be very difficult, because the time scales may be similar. This could lead to maximum achievable Q of 10-15.

A couple of alternative schemes for burn control, minor radius alterations and dynamic stabilization are tentatively discussed; no definite answers on their feasibility are obtained.

The problem of diagnosing the plasma with respect to burn conditions is the topic of chapter 5. The influence on the energy distribution of control actions and the reliability of neutron measurements are discussed, and the question of how to handle sawteeth is briefly revisited.

Chapter 6 is a description of process identification and how it could be used for burn control. It exists in different forms, and is already in use in fusion research. A particular advantage is that it can be combined with physical knowledge based on first principles. A couple of digital simulations of identification have been prepared and will soon be run.

Chapter 7, finally, is a brief description of our current plans.

References

1. T. Elevant, D. Anderson, H. Hamnén, M. Lisak, and H. Persson, "Pre-Study of Burn Control in NET", 1st Intermediate Report, CTH-IEFT/PP-1989-12, July 1989.
2. S.W. Haney, L.J. Perkins, and S.K. Ho, "ITER Operating Point Selection and Burn Stability Control", Lawrence Livermore National Laboratory (May 19, 1989).
3. J. Mandrekas and W.M. Stacey, "Evaluation of Different Control Methods for the Thermal Stability of ITER", Georgia Institute of Technology GFTR 92, (September 1989).
4. L. Bromberg, J.L. Fisher, D.R. Cohn, Nucl. Fus. 20 (1980) 203.

2. Introductory analysis of a simple zerodimensional system

2.1 Introduction

In order to deepen the insight into the thermal instability of a burning fusion plasma and its control the simplest possible, yet physically meaningful, zerodimensional system of equations has been considered. Linear analyses around different working points, with different assumed scaling laws, have been made. First, it has been assumed that there exists an independent control of the density, later the interplay between the n- and T-variations has been considered. In a number of cases, the nonlinear equations have been solved numerically. Straightforward control actions, based upon a variation of the injection of neutral particles, have been looked at, linearly and nonlinearly. The control is either P-, PD-, or state-space.

In the general, zerodimensional plasma evolution equations (See e.g. Ref. [1], we have assumed that

- the deuterium and tritium densities are equal. Control by for instance dilution may be looked into at a later stage.

- heavy impurities have only been regarded by their influence on Z_{eff} but their contribution to plasma charge balance, and energy losses by line radiation have been neglected.

- ohmic heating has been disregarded

- no details of the energy deposition from energetic alpha or neutral beam particles have been considered, including the distribution of energy to electrons and ions, or the delay in the deposition

- no magnetic compression is considered

2.2 Equations used

The equations become

$$\frac{dn}{dt} = S - \frac{n}{\tau_p}$$

$$\frac{3d(nT)}{dt} = P_\alpha + P_{aux} - P_b - \frac{3nT}{\tau_E} \qquad (1)$$

Here, S is the particle source term, P_α is the heat from fusion-generated alphas, P_{aux} the auxiliary heating power, and P_b the Bremsstrahlung loss. Use has been made of the standard assumption concerning the form of the energy and particle confinement times:

$$\tau_E = K_1 n^l T^m ; \quad \tau_p = K_2 \tau_E$$

Here, we expect that the interval [-4, 4] for l and m will cover all cases of interest. The constant K_2 is assumed to fulfil $1 \leq K_2 \leq 10$, typically, a value $K_2 = 3$ has been chosen.

The multiplicative constant K_1 is kept as one of the parameters of the problem. When a particular scaling law is applied to a particular machine, like NET or ITER, K_1 will get a particular numerical value.

At the working point (index 0), the LHS in (1) become zero. Subtracting the resulting equations from (1), we obtain

$$\frac{dn}{dt} = (S - S_o) - \left(\frac{n}{\tau_p} - \frac{n_o}{\tau_{p,o}}\right)$$

$$3\,\frac{d(nT)}{dt} = (P_\alpha - P_{\alpha,o}) + (P_{aux} - P_{aux,o}) - (P_b - P_{b,o}) -$$

$$-\left(\frac{3nT}{\tau_E} - \frac{3n_oT_o}{\tau_{E,o}}\right) \qquad (2)$$

In the case of an uncontrolled plasma (an "open system"), the supply of particles and the auxiliary heating are kept at the values corresponding to the working point:

$$S - S_o = 0\,; \quad P_{aux} - P_{aux,o} = 0$$

A change of units is made: particle temperatures are given in keV, and densities in units of $10^{20}/m^3$. Transforming the equations accordingly, and dividing the energy equation by 3, we obtain the following system for the dynamics of the uncontrolled plasma:

$$\frac{dn}{dt} = -\left(\frac{n}{\tau_p} - \frac{n_o}{\tau_{p,o}}\right)$$

$$\frac{d(nT)}{dt} = (P_\alpha - P_{\alpha,o}) - (P_b - P_{b,o}) - (P_f - P_{f,o}) \qquad (3)$$

Here, the transformed Bremsstrahlung losses are given by

$$P_b = 0.1\, n^2 \sqrt{T}\, Z_{eff}\ ;\ \text{typically}\ 1.3 \leq Z_{eff} \leq 5$$

For P_α, approximated by one fifth of the fusion power, we adopt a formula based on the expression S_5^{**} of Hively [2], for the reactivity. This is claimed by the author to be accurate within a few per cent, up to 80 keV. We get

$$P_\alpha = 2.917 \times 10^{16}\, n^2 \exp\left(\frac{a_1}{T^r} + a_2 + a_3 T + a_4 T^2\right)$$

where $a_1 = -\ 20.779964$

$a_2 = -\ 25.813871$

$a_3 = -\ 6.625135 \times 10^{-2}$

$a_4 = \ \ 3.0934551 \times 10^{-4}$

$r = \ \ 0.30366647$

Furthermore,

$$P_f = \frac{nT}{K_1\, n^l\, T^m}$$

Pertinent equilibrium temperatures are believed to lie between 8 and 25 keV, and densities between 0.5 and 5, with the units chosen.

For a subignited plasma, we shall most of the time use the Q-value at the working point,

$$Q_o = \frac{P_{fus,o}}{P_{aux,o}} \approx \frac{5\, P_{\alpha,o}}{P_{aux,o}}$$

instead of the multiplicative constant K_1. This is because Q_o is felt to be a more illustrative physical and technical quantity. The equilibrium energy balance condition furnishes the simple relation between those two numbers:

$$K_1 = \frac{1}{n_o^{l-1} T_o^{m-1} \left(P_{\alpha,o} \left(1 + \frac{5}{Q_o} \right) - P_{bo} \right)}$$

Q_o can be expressed as

$$Q_o = \frac{5 P_{\alpha o}}{P_{bo} - P_{\alpha o} + \frac{1}{K_1 n_o^{l-1} T_o^{m-1}}}$$

Typically, we have $1 \leq Q_o \leq \infty$.

2.3 Stability against pure temperature variations

To study the temperature instability in the simplest possible way, it may be instructive to assume that the density is maintained at its working point value, $n = n_0$, by a separate density control system. We then only need to consider temperature variations. The faster time scale of the energy variation than that of the density may be an argument in favour of this view.

Dividing the energy equation by the constant density, we may write

$$\frac{dT}{dt} = F(T)$$

The stability is analysed by linearizing around an equilibrium T_0, $F(T_0) = 0$.

$$F(T) \approx (T - T_0) \cdot F'(T_0)$$

Integration then gives

$$T - T_o = [T(0) - T_o] \cdot e^{F(T_o)\cdot t}$$

where T(0) is the temperature at time zero. Clearly, we have exponential growth or decay of a perturbation, according to whether $F'(T_o) > 0$ or $F'(T_o) < 0$.

Inserting the actual expressions and differentiating, we get

$$F'(T_o) = \frac{P_{\alpha,o}}{n_o}\left(-\frac{r a_1}{T_o^{r+1}} + a_3 + 2a_4 T_o\right) - 0.05\, n_o \frac{Z_{eff}}{\sqrt{T_o}} - \frac{(1-m)}{K_1 n_o^l T_o^m}$$

The first term corresponds to the tendency towards growth, due to the alpha particle heating, and the second to the (modest) stabilizing influence of the Bremsstrahlung (e.g., with $Z_{eff} = 2$; $T_o = 10$ keV; $n_o = 1$ ($\cdot 10^{20}/m^3$), the Bremsstrahlung time constant becomes 32 seconds). We observe that the influence of the last term, from transport, becomes marginal for m = 1. For larger values of m, it becomes destabilizing; this is then due to an energy confinement that is sufficiently much improved when the temperature goes up.

Summing up the different contributions, we conclude that the conditions for stability against purely thermal perturbations, with the density assumed to be constant becomes

$$\frac{P_{\alpha,o}}{n_o}\left(-\frac{r a_1}{T_o^{r+1}} + a_3 + 2\, a_4 T_o\right) - 0.05\, n_o \frac{Z_{eff}}{\sqrt{T_o}} - \frac{(1-m)}{K_1 n_o^l T_o^m} < 0 \qquad (4)$$

This gives a limitation on the magnitude of the multiplicative constant K_1, or, alternatively, on the magnitude of Q_o.

A simple program code (LOCAL2) has been written that calculates the characteristic times corresponding to the various terms in $F'(T_o)$, as well as

the value of $1/F'(T_o)$. Furthermore, it gives the highest possible Q_o-value for which the burn is thermally stable in the present sense. It also generates the eigenvalue and eigenvector information to be described in the next paragraph.

2.4 Stability against coupled temperature and density variations

Without assuming the density to be constant, the coupled variation of n and T has been studied in the linear approximation, using elementary theory of differential equations [3]. The system behaviour around a working point (n_o, T_o) is then characterized by a matrix of the partial derivatives of the right-hand members, evaluated at the working point. Specifically with

$$\frac{dn}{dt} = f_1 (n, T; \text{parameters})$$

$$\frac{dT}{dt} = f_2 (n, T; \text{parameters})$$

we get

$$(A_{ik}) := A = \begin{pmatrix} \left(\frac{\partial f_1}{\partial n}\right)_o & \left(\frac{\partial f_1}{\partial T}\right)_o \\ \left(\frac{\partial f_2}{\partial n}\right)_o & \left(\frac{\partial f_2}{\partial T}\right)_o \end{pmatrix}$$

The topological character of the solutions in the vicinity of (n_o, T_o) is then obtained from the eigenvalues of this matrix, and stable and unstable manifolds of saddle points or fast and slow manifolds of nodes are obtained from the eigenvectors.

To implement this, in the second equation of the system (3), we differentiate the product, subtract T dn/dt, using the expression for dn/dt in the first equation, and divide by n. We then obtain the system

$$\frac{dn}{dt} = -(F_p - F_{p,o})$$

$$\frac{dT}{dt} = \frac{P_\alpha - P_{\alpha,o}}{n} - \frac{P_b - P_{b,o}}{n} - \frac{P_f - P_{f,o}}{n} + \frac{T}{n}(F_p - F_{p,o}) \qquad (5)$$

where $F_p = \frac{n}{\tau_p}$.

Differentiating, we obtain after some algebra

$$A_{11} = \frac{l-1}{\tau_p}\,; \quad A_{12} = \frac{m\, n_o}{T_o\, \tau_p}\,;$$

$$A_{21} = 2\,\frac{P_{\alpha o} - P_{bo}}{n_o^2} + \frac{T_o}{n_o}(l-1)\left(\frac{1}{\tau_E} - \frac{1}{\tau_p}\right);$$

$$A_{22} = \frac{P_{\alpha o}}{n_o}\left(-\frac{a_1 r}{T_o^{r+1}} + a_3 + 2a_4\, T_o\right) - \frac{P_{bo}}{2n_o T_o} - \frac{l-m}{\tau_E} - \frac{m}{\tau_p}$$

In A_{22} we recognize the earlier used quantity $F'(T_o)$, but there is also an additional, stabilizing (for $m > 0$) contribution from the energy loss by particle transport.

The quantities decisive for stability are the trace and the determinant of this matrix:

$$\text{Trace: } = A_{11} + A_{22}$$

$$\text{Det: } = A_{11}A_{22} - A_{12}A_{21}$$

The stability condition becomes [3]

$$\begin{cases} \text{Trace} < 0 \\ \text{Det} > 0 \end{cases}$$

If it is fulfilled, one either gets two negative eigenvalues, in which case the working point is a stable node, or two complex roots with a common, negative real part, corresponding to a stable spiral. The choice between real and complex eigenvalues is given by discriminant

$$\text{Disc:} = \text{Trace}^2 - 4\,\text{Det}$$

and the eigenvalues may be written

$$\lambda = \frac{\text{Trace} \pm \sqrt{\text{Disc}}}{2}$$

The earlier mentioned code (LOCAL2) also calculates these eigenvalues and the corresponding eigenvectors, for arbitrary working points (n_o, T_o), physically allowable Q_o-values, and various assumptions (l, m) on the scaling law. This has been made in a number of cases.

In general, these eigenmodes include a variation of both n and T, but in some cases, notably for m = 0, one eigenvector is parallel to the T-axis.

Many cases have been observed, in which a pure T-variation is stable, but where the added degree of freedom by allowing n to vary gives instability in the phase plane. It appears that a fairly accurate constancy of n would be necessary in order to suppress thermal instability in these cases.

2.5 Nonlinear numerical calculations

The system of equations (5), describing the nonlinear evolution of the uncontrolled plasma in nT-space, has been solved numerically in a number of cases. The "DOPEX" program package by Dahlqvist and Littmarck [4] has

been used, which includes a Turbopascal translation of the Fortran code of Hairer, Norsett and Wanner [5], implementing the optimized Runge-Kutta algorithm of Dormand and Prince [6].

In Figs. 1-3, the burn instability is nicely demonstrated. There are exceptional cases with intrinsically stable burn (see Figs. 4a-c), but in general feedback control must be applied. The case of the scaling l=2; m=0, is quite interesting. Since the confinement improves strongly with increasing density, there is an unstable development of the density, and in Fig. 2, with a high Q-value of 30, the density instability is more striking than the temperature instability, especially for high n. With an initial point to the right of and below the working point, T first goes down a little, while n increases to a not very well defined value, at which the density stays essentially constant, while T rushes upwards.

Fig. 3 is but one of many examples when the temperature varies stably for $n = n_0$, but where any density deviation will lead to an unstable development of both n and T.

Attempts have been made to stabilize unstable burn by feedback control, with a variation of the supply of fast neutral particles. This then both involves a modulation of the source of particles and of the auxiliary heating.

Putting the additional term in the right-hand member of the particle balance equation in (2) equal to δS:

$$\delta S \equiv S - S_o$$

δS will show up in the corresponding equation in (5). The temperature balance equation in (5) hereby gets an extra term

$$\frac{E_o/3 - T}{n}\,\delta S$$

Here, E_o is the neutral particle energy; the factor 3 is due to the division by 3 used to arrive at (5).

In the simplest possible case, we try a control proportional to the deviations of n and T from their values at the working point. In this preliminary exercise, all delays are neglected, and it is assumed that both density and temperature are measured and used for the control:

$$\delta S = -\alpha(n-n_o) - \beta(T-T_o)$$

The constants α and β are then to be determined to give the closed system "good" properties.

In the linear approximation additional terms are obtained. Let us by primed quantities identify those obtained, with control applied.

Differentiation gives

$$A'_{11} = A_{11} - \alpha\,;\quad A'_{12} = A_{12} - \beta$$

$$A'_{21} = A_{21} - \frac{E_o/3 - T_o}{n_o}\,\alpha$$

$$A'_{22} = A_{22} - \frac{E_o/3 - T_o}{n_o}\,\beta$$

This then also gives expressions for the new trace Trace' and determinant Det'.

The further analysis of the closed system shows that it is always possible to stabilize the situation linearly. A pole location of + and - 135 degrees

has been used; this is an often used location giving a time variation in the linear approximation of

$$e^{\lambda t}(A \cos \lambda t + B \sin \lambda t)\,;\ \lambda < 0$$

which is often suitably much oscillatory. This is obtained by putting Det' = $2\lambda^2$, Trace' = 2λ. One gets a linear system of equations for α and β, which can be solved and expressed in the old matrix A and λ. It turns out that λ can be chosen essentially at will.

In a practical situation, determinations of average density and temperature may take too long time to carry out. Therefore, we have looked into the possibilities of instead using the neutron flux, which is proportional to the P_α-signal. We then put $\delta S = - K(P_\alpha - P_{\alpha o})$. The additional terms appearing in the linear analysis now involve the partial derivatives of P_α with respect to a and T. There is one parameter less at hand than in the preceding problems, but one may try to locate the poles at + and -135 degrees. This leads to a second degree equation for λ, which may or may not have negative solutions.

A number of examples of feedback control have been run. We have assumed E_o = 300 keV. This is still ongoing work; here, we mainly wish to illustrate the Q_o-limitation analysed in chapter 4. Fig. 5a shows the unstable working-point/scaling law $n_o = 1; T_o = 18$; $Z_{eff} = 2$; $Q_o = 50$; l = 1; m = 0.1. If there were no limitations on the NBI-injection swing, we would have the well-controlled situation shown in Fig. 5b. The NBI modulation is determined by the deviations in density and temperature. The poles have been placed at - 0.2 ± 0.2i. However, imposing the condition $P_{aux} \geq 0$, we obtain the diagram in Fig. 5c. The thermal runaway is clearly shown, especially for high initial densities. In spite of the high Q_o-value of 50, however, the control system can handle a 20% pure T-perturbation (curve A in the figure), but it appears as if a 25% perturbation (curve B) would lead to a temperature excursion.

The same curves have also been produced for $Q_0 = 10$. In this case, they are identical to each other within the nT-window shown; thus more than a 33% positive δT can readily be handled in this case.

This underlines that the phenomenon is important. Qualitatively, the linear, simplified analysis does not give accurate answers. The discrepancy may be due to the interplay between n and T and/or the nonlinearity.

The same curves have also been produced with control based on the P_α-signal, ($Q_0 = 50$). The "best" 135-degree feedback then gives poles at -0.1954 ± 0.1954 i. Clearly, the linear approximation is almost identical with the previous case. Nonlinearly, the diagrams are quite similar.

With $l = 2$, the density tends to be quite unstable. It is still possible, in the linear approximation, to find suitable pole locations, but the nonlinearities become quite strong. In some cases, the region of validity may shrink to about 1%. Outside this region, the plasma is still unstable.

This difficulty seems to express the fact that with $l = 2$, we get a strongly unstable density, and injection of energetic neutral particles only is an inefficient way of influencing the density; the temperature gets too much upset.

2.6 Work in progress

There are some natural extensions of the work just reported. A machinery for analyzing unstable burn and its control has been built up and tested, and work with its application to several other cases is under way. Specifically, the linear stability analyses should be carried out for more situations. The stability conditions found on Q_0 should be presented in a clear way, using suitable graphic representations. One would then both represent the condition on the working point for different scaling laws, as

well as conditions on the scaling laws for a number of selected working points, among which those of ITER will be found.

Once the differential equations have been solved, it is easy and straightforward to compute additional curves of technical and physical interest, e.g., fusion power, additional heating power, Q-value, etc. as functions of time. Whenever the magnetic field strength is given, a beta limit, e.g. that of Troyon, can readily be introduced into the diagram.

Work on a code for POPCON construction has been started; it will in the present model not include any sophistication regarding different heating of electrons and ions [7].

2.7 Plans for the future

In addition to the items described in the paragraph 2.6 the plans include the following aspects.

The study of the P_α-signal as a basis for control should be pursued. The natural continuation seems to be to reconstruct the "state" of the plasma; e.g. as given by n and T, using what in control theory is called an "observer", a procedure for estimating the state of the system from input and output. This is then combined with state-space control.

Especially for high energy of the injected particles, and for scaling laws giving rise to a strong density instability, a combination of changes in the neutral beam injection and the supply of gas or pellets has to be used. This has been illustrated in one of the examples above. An optimum choice of control actions for these two actuators will then have to be based upon a suitable principle of optimization.

It is well-known [8] that minimizing the integrated quadratic error with bounds on the absolute value of the control signal leads to control algo-

rithms that are either nonlinear or explicitly time-dependent. However, linear-quadratic optimization is still at hand; a suitable functional to be minimized by chosing the linear approximation to the controlled system may be of the form

$$\int_0^\infty [\alpha_1 y^2(t) + \alpha_2 u^2(t)]dt\,; \quad \alpha_1 > 0\,; \quad \alpha_2 > 0$$

where u is the input and y the output. It is expected that one will also have to study the optimization on the basis of the full, nonlinear system.

The choice of α_1 and α_2 will involve questions of technical judgement concerning the desirability of avoiding excessive or long-time deviations of n and T from their proper values, in comparison with the power and energy restrictions on the actuators. Generally, these judgements have to appear in close contact with the NET/ITER team; at the present time our ambition is to provide options, between which it is possible to choose.

A burning fusion plasma is expected to be partially known and understood theoretically, partially unknown, particularly with respect to its transport scaling laws. This suggests use of process identification as a basis for the description and control of the plasma and for determining values of unknown parameters. This will be further discussed in Sec. 6, here we only wish to point out that the empirical element of process identification can be elegantly combined with the theoretical knowledge at hand.

References

1. T. Elevant, D. Anderson, H. Hamnén, M. Lisak, and H. Persson, "Pre-Study of Burn Control in NET", 1st Intermediate Report, CTH-IEFT/PP-1989-12, July 1989.
2. L.M. Hively, "Convenient Computational Forms for Maxwellian Reactivities", Nucl. Fus. 17 (4) (1977) 873.
3. G. Strang, in "Introduction to Applied Mathematics", Wellesley-Cambridge Press, (1986), pp. 492-503.
4. G. Dahlqvist and S. Littmarck, private communication.
5. E. Hairer, S.P. Norsett and G. Wanner, in "Solving Ordinary Differential Equations", Vol. I, Springer-Verlag (1987), pp. 171-184, 433-435.
6. J.R. Dormand and P.J. Prince, "A Family of Embedded Runge-Kutta Formulae", Comp. Appl. Math. 6 (1980), pp. 19-26.
7. J. Mandrekas and W.M. Stacey, "Evaluation of Different Control Methods for the Thermal Stability of ITER", Georgia Institute of Technology, GFTR 92, (September 1989).
8. C.T. Chen, in "Analysis and Synthesis of Linear Control Systems", Holt, Rinehart and Winston, Inc. (1975), pp. 185-187.

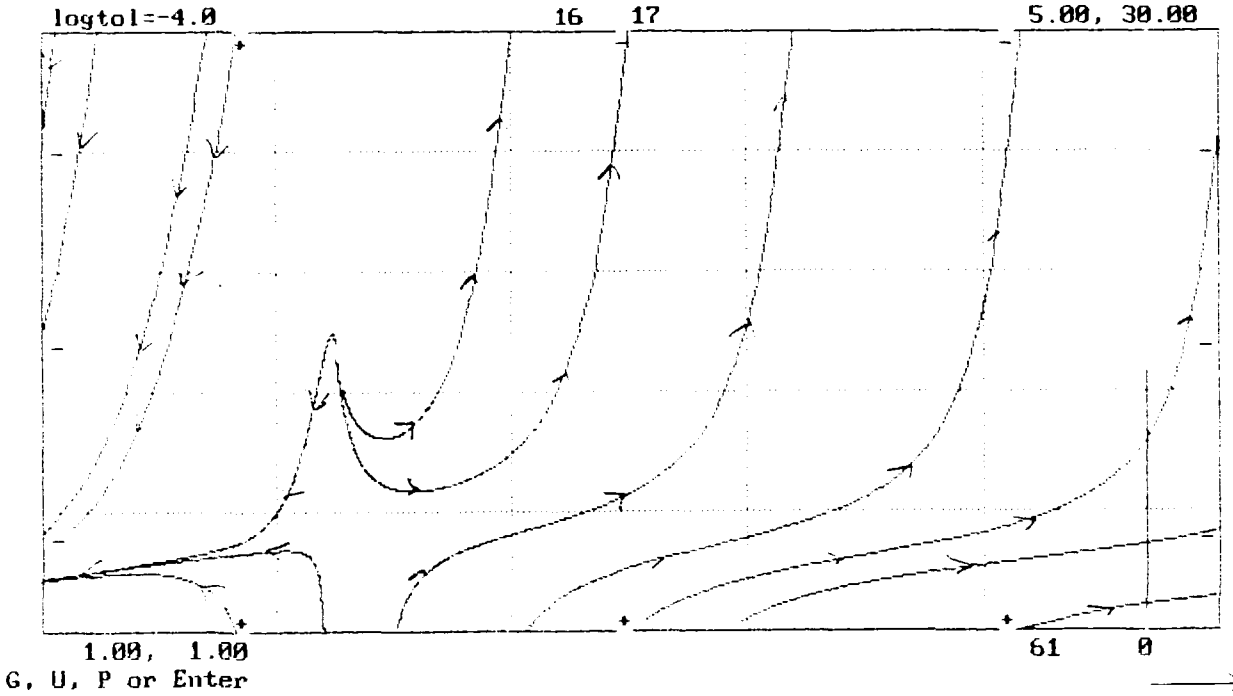

Fig.1. Phase plane trajectories for an uncontrolled plasma, (n_o = 2; T_o = 15; Z_{eff} = 2; Q_o = 10; l = 2; m = 0).

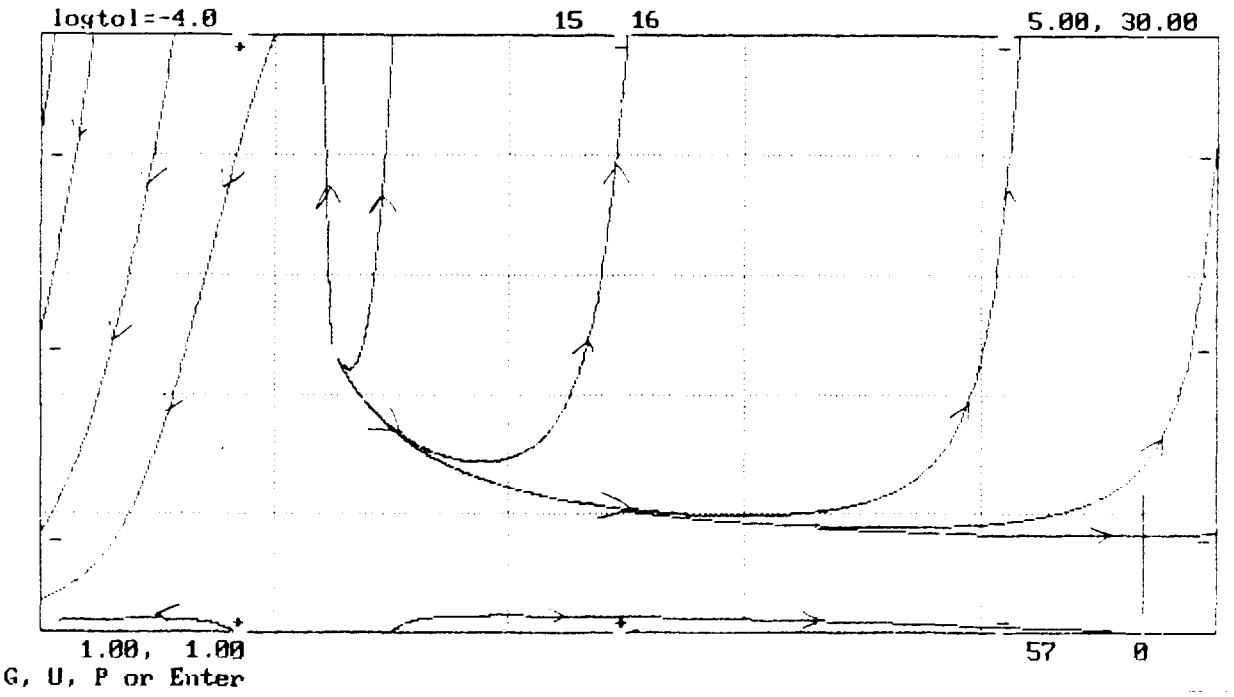

Fig. 2. Same diagram as in Fig. 1, but with Q_o = 30.

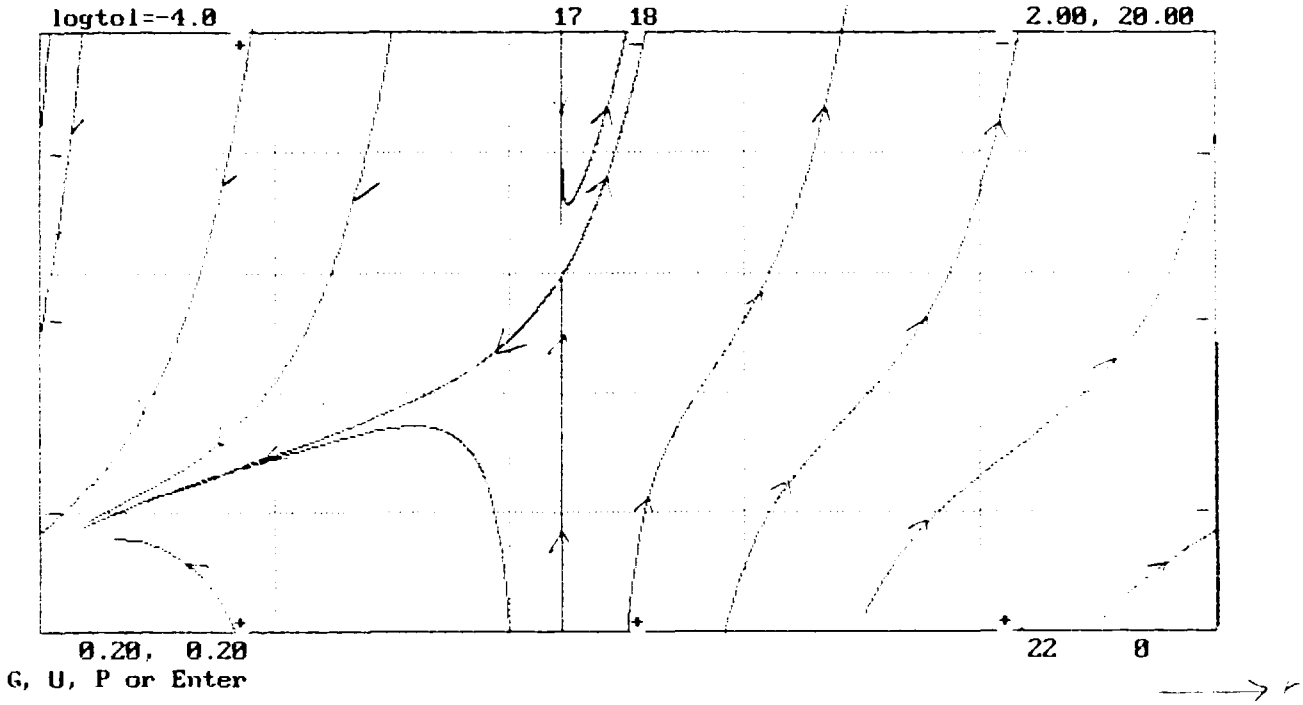

Fig. 3. nT-diagram (n_o = 1; T_o = 12; Z_{eff} = 3; Q_o = 3; l = 2, m = 0): uncontrolled plasma.

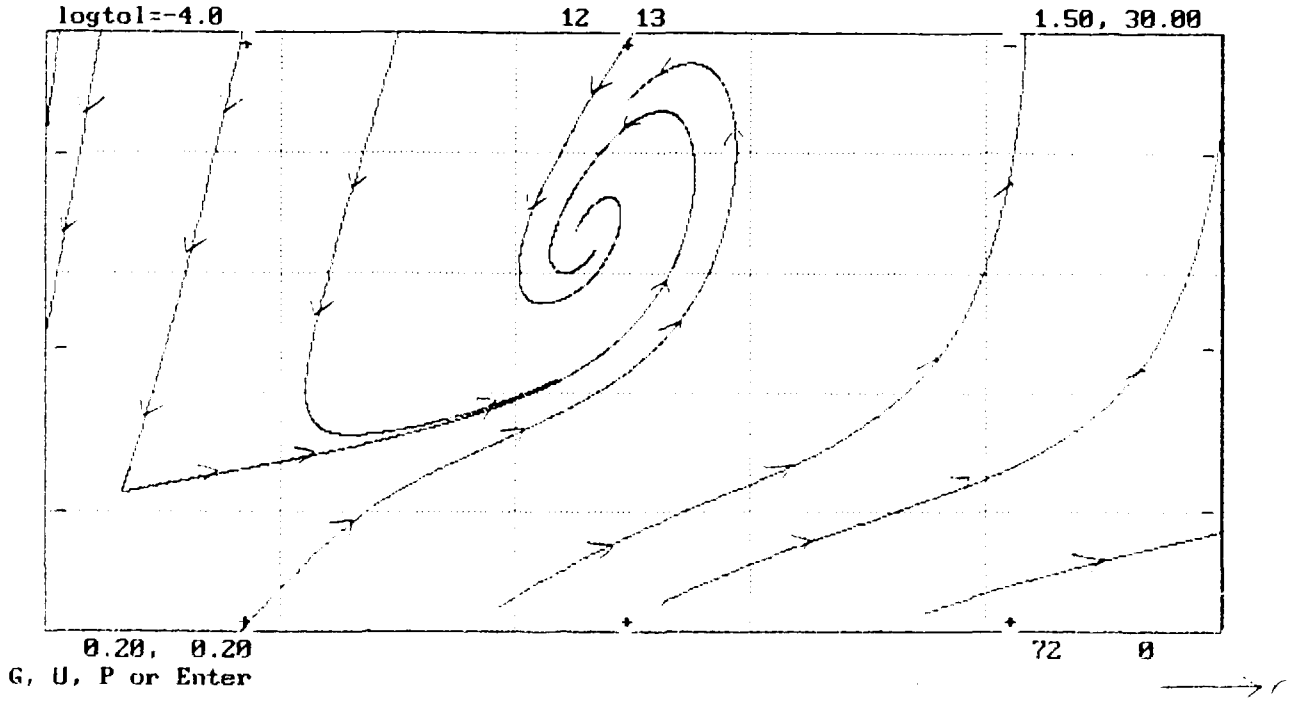

Fig. 4a. Phase plane diagram of an intrinsically stable plasma (n_o = 0.8; T_o = 20; Z_{eff} = 2; Q_o = 10; l = 2; m = -1).

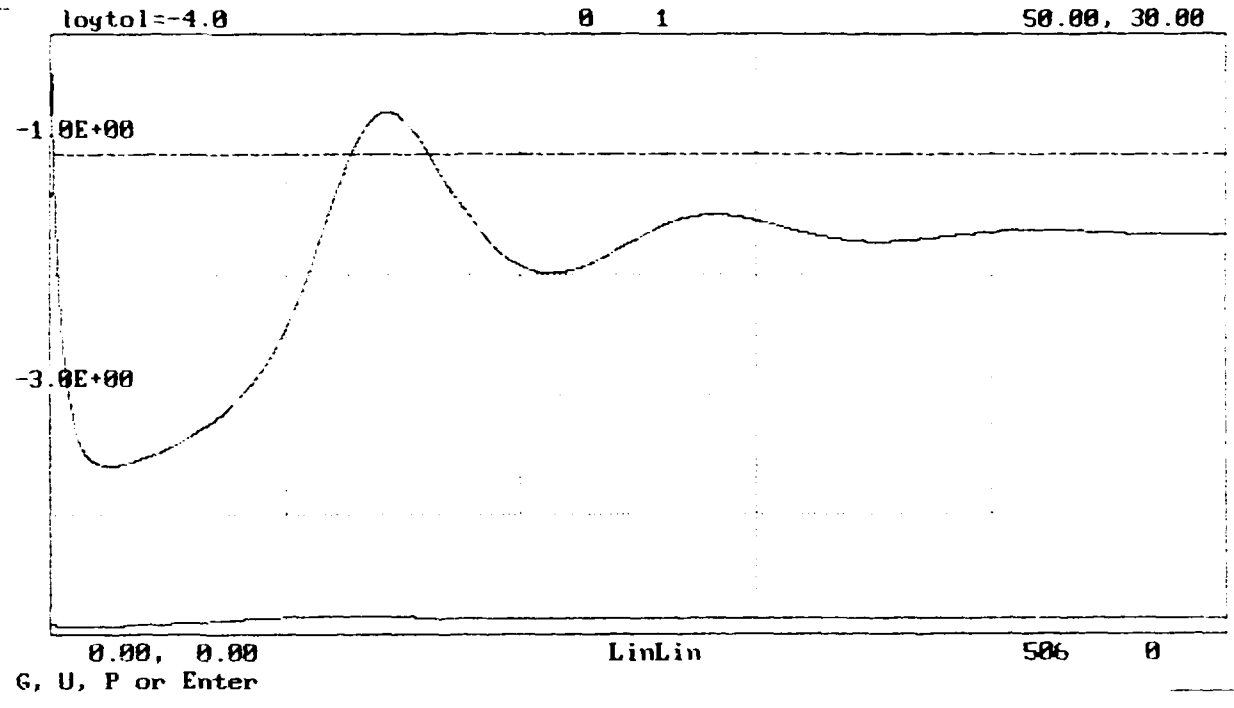

Fig. 4b. T(t) (and n(t)) for this case; n(0) = 0.5; T(0) = 30.

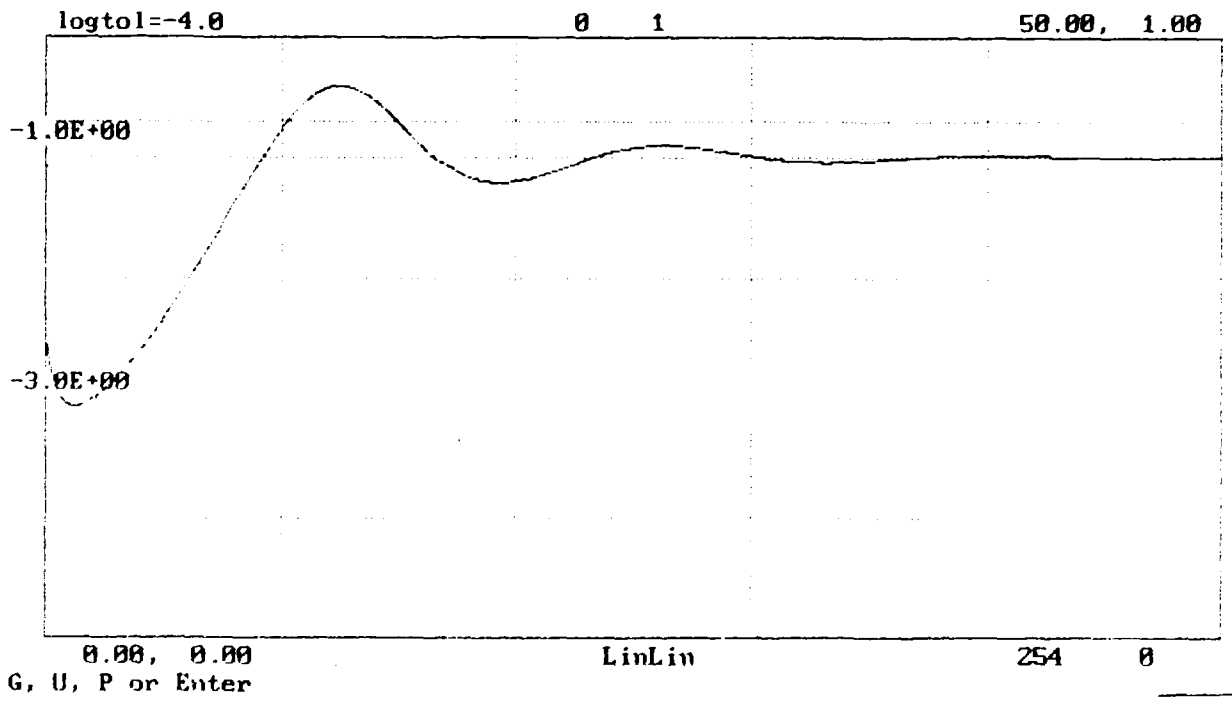

Fig. 4c. n(t) for this case.

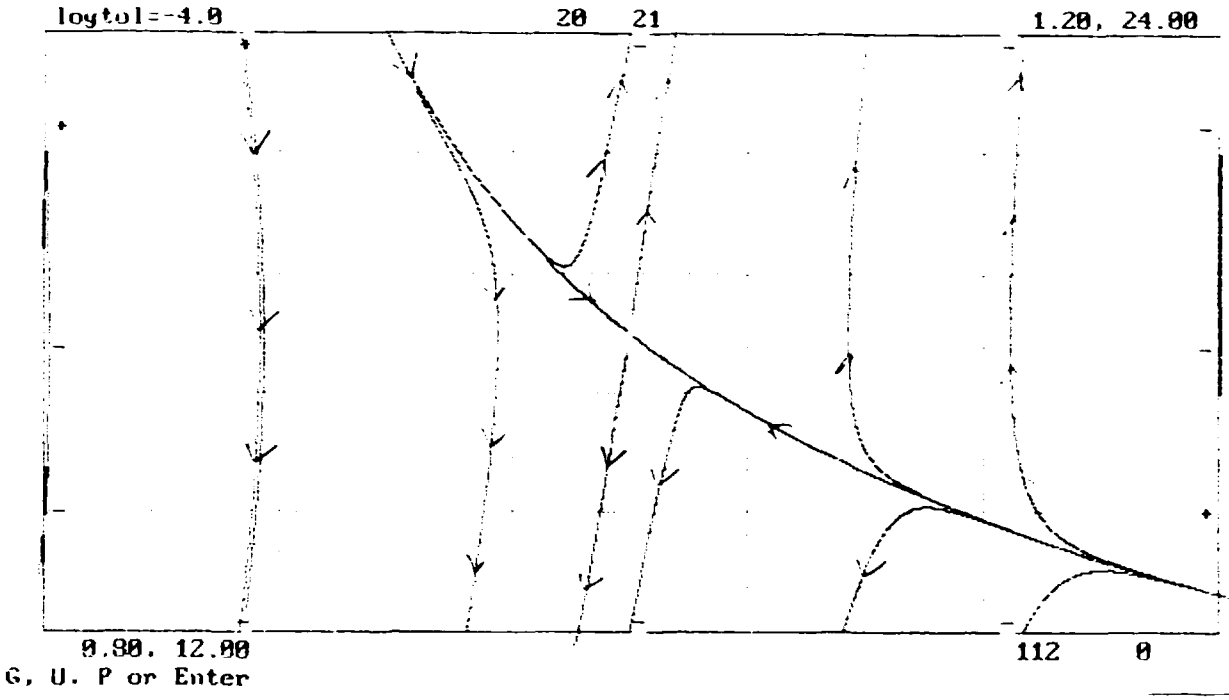

Fig. 5a. Uncontrolled plasma (n_O = 1; T_O = 18; Z_{eff} = 2; Q_O = 50; l = 1; m = 0.1).

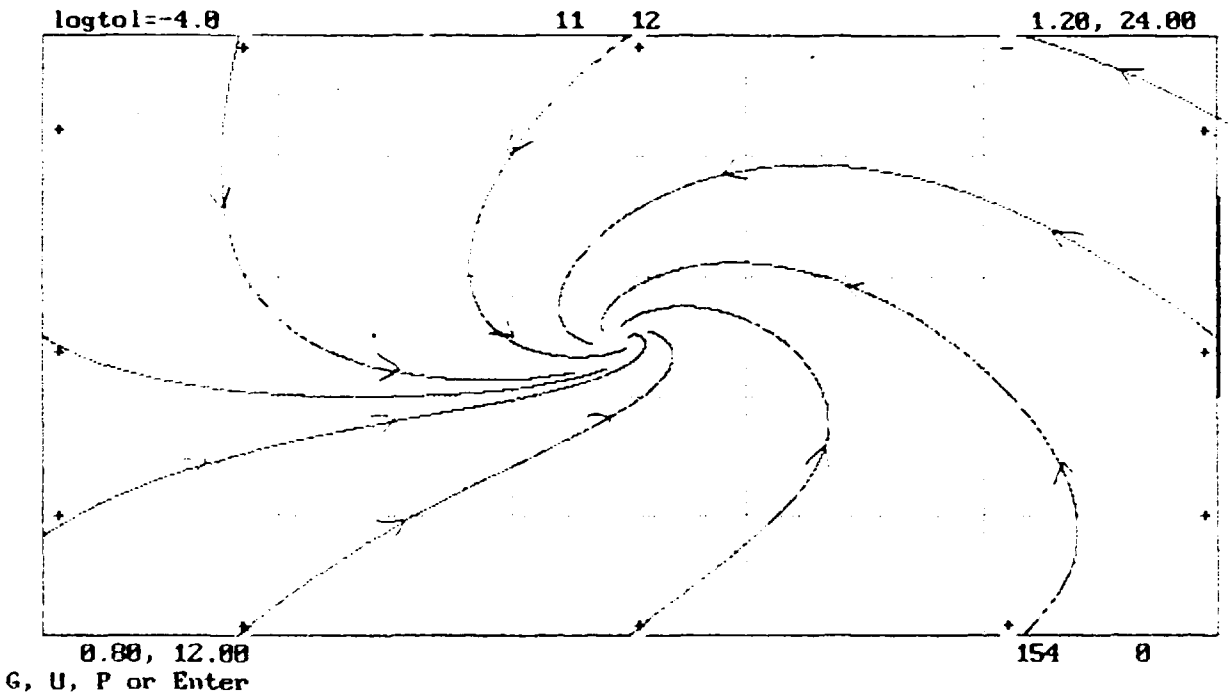

Fig. 5b. Controlled plasma, (proportional control based on the n and T signals) disregarding limited NBI swing.

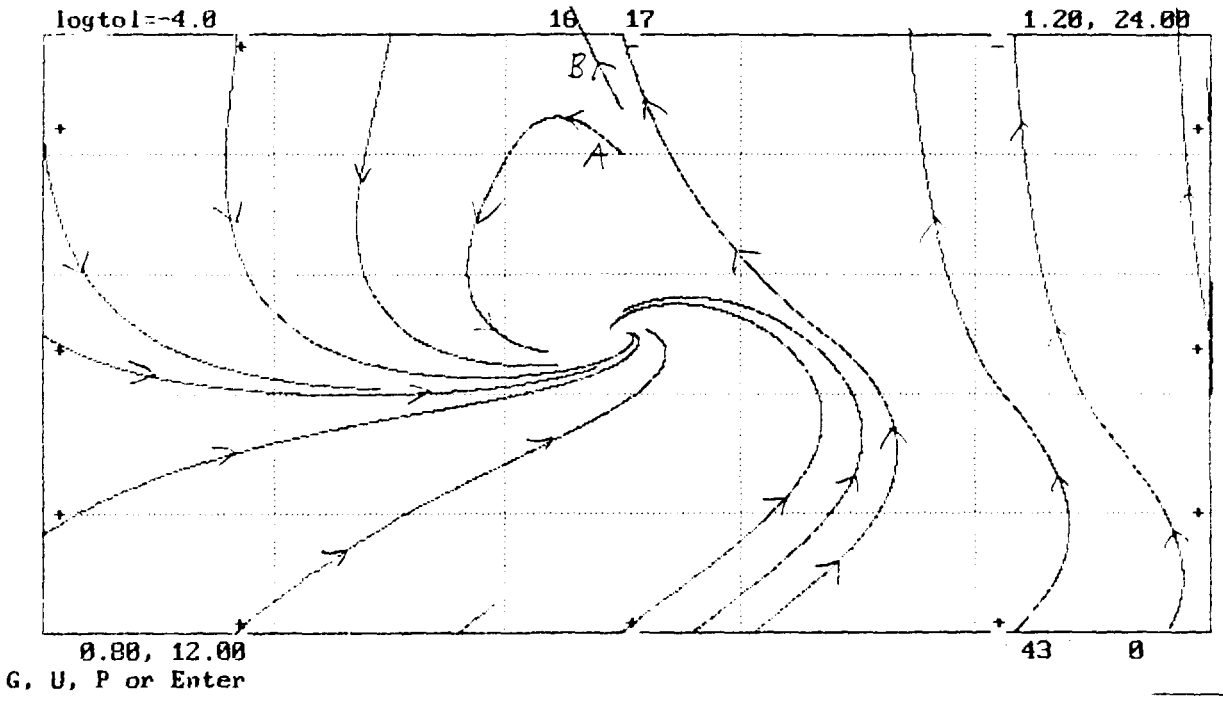

Fig. 5c. Controlled plasma with NBI limitations included.

3. Approximate analysis of the energy balance equation of a burning fusion plasma

3.1. Introduction

In an ignited DT fusion plasma, the plasma temperature is sustained against power losses by the collisional heating during slowing down of the fusion produced alpha particles. The corresponding plasma energy balance equation is strongly nonlinear and in general allows for two different equilibrium solutions corresponding to a "low" temperature and a "high" temperature mode of operation. Technical and physical constraints favour the low temperature equilibrium, at temperatures $T > 10$ keV, even though this equilibrium is unstable to temperature perturbations and must be stabilized by external control mechanisms [1].

A significant effort has been made to study the heating to burn, the subsequent equilibrium and stability properties of the burning plasma, and possible means of stabilization [1,2]. Most of these efforts have been based on 0-D models or extensive numerical codes to describe the space dependence of plasma parameters like density and temperature. Furthermore the 0-D modelling is often done in a heuristic way, which does not clearly relate to the space dependent equations. The purpose of the present work is to put the approximation procedure involved in the transition to 0-D models on a more formal basis. Secondly, simple and useful approximations of the radial equilibrium temperature profiles will be derived for a class of nonlinear transport and heating models. These approximations should be useful, e.g. when investigating various schemes for feedback control of the equilibrium. The 1-D equilibrium solution is also investigated with respect to its stability properties, which are shown to be the same as those derived from the simplest 0-D space averaged model.

Finally, an application of the approximate solution is made to determine the equilibrium properties for a particular transport model.

3.2 Thermal balance equation

The basic mechanism for thermal equilibrium and stability of a fusion reactor plasma can be understood by considering the energy balance equation:

$$\frac{\partial}{\partial t}(3nT) = P_s - P_l \qquad (1)$$

where n is the plasma density, T is the plasma temperature, and P_s and P_l denote the heating power and the power loss respectively. Planned operation temperatures in future DT Tokamak reactors are restricted by β-limitations to be T > 10 keV. In this temperature range P_s and P_l are dominated by alpha particle deposition heating and transport losses respectively, i.e.

$$P_s = \frac{n^2}{4} \langle \sigma v \rangle E\alpha = P_\alpha$$

$$-P_l = \frac{1}{r}\frac{\partial}{\partial r}\left(mn\kappa \frac{\partial T}{\partial r}\right) \qquad (2)$$

where $\langle \sigma v \rangle$ is the DT reaction rate, E_α = 3.5 MeV, and κ is the thermal conductivity.

The reaction rate, which depends strongly on temperature, is modelled as $\langle \sigma v \rangle \sim T^p$, where p = d ln $\langle \sigma v \rangle$/d lnT. The power law exponent, p, decreases with increasing temperature, cf Figs. 1 and 2.

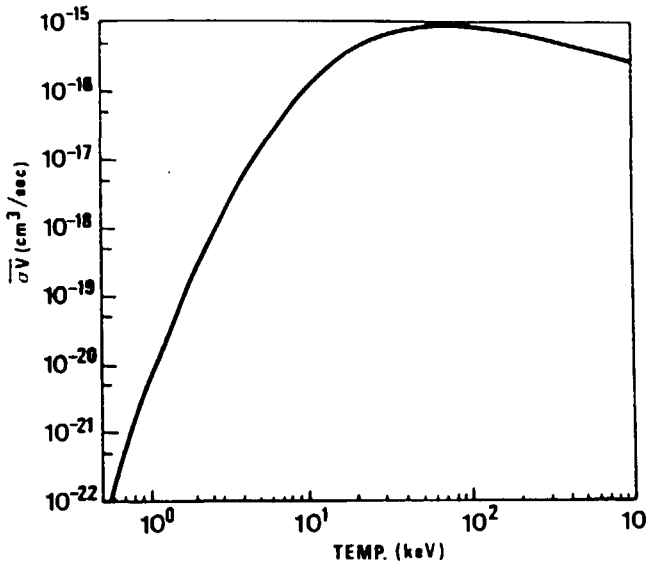

Fig. 1. Fusion rate <σv> for a thermal fusion plasma.

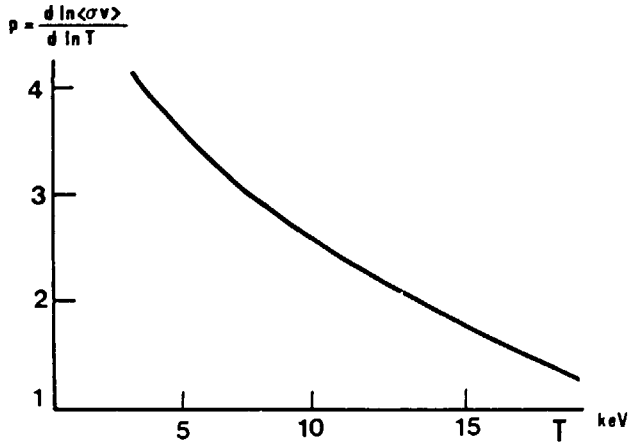

Fig. 2. The power law exponent for <σv>, viz. p = dln<σv>/dlnT as a function of temperature.

A crucial problem in present-day fusion plasma research is the proper modelling of κ and the extrapolability of these models to fusion reactor conditions. In the present analysis we will approximate the temperature dependence of κ in the form of a power law: $\kappa \sim T^{\delta}$. For simplicity we will first assume the density, n, to be constant in time as well as in space. With these restrictions eq. (1) can be written

$$\frac{\partial T}{\partial t} = \frac{1}{r}\frac{\partial}{\partial r}\left(r\frac{\kappa}{3}\frac{\partial T}{\partial r}\right) + S \qquad (3)$$

The evolution of the temperature T(r,t) is subject to the boundary conditions

$$\frac{\partial T}{\partial r}(0,t) = 0$$

$$T(a,t) = 0 \qquad (4)$$

where a denotes the plasma minor radius.

3.3. Space-averaged analysis

Most investigations of the problem of igniting and then controlling the subsequent burn of a fusion reactor plasma have relied on 0-dimensional simplifications of more or less complete dynamic plasma equations [2]. Eq. (3) represents the simplest dynamic equation modelling the self-sustained burn of a fusion reactor plasma.

Generally, the reduction of the system to eliminate the space dependence can be done in a heuristic way by replacing the effect of the diffusion operator in eq. (3) with an energy confinement time, τ_E, according to

$$\frac{1}{r}\frac{\partial}{\partial r}\left(r\frac{\kappa}{3}\frac{\partial T}{\partial r}\right) \rightarrow -\frac{T}{\tau_E} \qquad (5)$$

where $\tau_E = 3L_{eff}^2/\kappa$ and L_{eff} is an effective radius of the order of the plasma minor radius a. We will begin our investigation by demonstrating a formal averaging procedure, which reduces eq. (3) to a time dependent problem for the average temperature. The confinement time can then be given explicitly in terms of the properties of the averaged quantities and the properties of the thermal conductivity. The system is then easily analyzed for equilibrium and stability.

In order to space average eq. (3), an assumption about the temperature profile must be made. A convenient model compatible with the boundary conditions, is $T = T(0)\ (1-r^2/a^2)^{\alpha}$. Define a formal averaging procedure as

$$\langle f \rangle \equiv \frac{2}{a^2} \int_o^a rf\, dr \tag{6}$$

and apply it to eq. (3). This yields

$$\frac{d\langle T \rangle}{dt} = - \bar{K}_o \langle T \rangle^{\delta+1} + \bar{S}_o \langle T \rangle^{P} \tag{7}$$

where $\bar{K}_o$ and $\bar{S}_o$ are defined by

$$\frac{\kappa}{3} = K_o T^{\delta}$$

$$S = S_o T^{P} \tag{8}$$

together with

$$\left\langle \frac{1}{r} \frac{\partial}{\partial r} \left(r K_o T^{\delta} \frac{\partial T}{\partial r} \right) \right\rangle = - \frac{4K_o}{a^2} \frac{(\partial+2)^{\delta+1}}{(\delta+1)^{\delta+2}} \langle T \rangle^{\delta+1} \equiv - \bar{K}_o \langle T \rangle^{\delta+1}$$

$$\langle S_o T^{P} \rangle = \frac{S_o}{p+\delta+1} \frac{(\delta+2)^{P}}{(\delta+1)^{P-1}} \langle T \rangle^{P} \equiv \bar{S}_o \langle T \rangle^{P} \tag{9}$$

In deriving eqs. (8) and (9) we have made use of the fact that the averaging of the diffusion yields a finite result only if $\alpha = 1/(\delta+1)$. This implies that the thermal conductivity has a dominating influence on the temperature profile, much stronger than the heating term. Note in particular that the profile peaking factor, R, is determined solely by the power law exponent of the thermal conductivity, viz. $R = T(0)/\langle T \rangle = (\delta+2)/(\delta+1)$.

Comparing with eq. (5) we identify the confinement time as

$$\tau_E = \frac{a^2}{4K_o\langle T\rangle^{\delta}} \frac{(\delta+1)^{\delta+2}}{(\delta+2)^{\delta+1}} \tag{10}$$

i.e.

$$L_{eff}^2 = \frac{a^2}{4} \frac{(\delta+1)^{\delta+2}}{(\delta+2)^{\delta+1}} \tag{11}$$

The equilibrium solution of eq. (7) is

$$\langle T_S\rangle = \left(\frac{\bar{S}_o}{\bar{K}_o}\right)^{\frac{1}{\delta+1-p}} \tag{12}$$

The stability of the equilibrium solution is determined by the linearized equation for the perturbation $\Delta\langle T\rangle$, viz.

$$\frac{d\Delta\langle T\rangle}{dt} = \frac{\partial H}{\partial\langle T_s\rangle} \Delta\langle T\rangle \tag{13}$$

where

$$H = \bar{K}_o\langle T\rangle^{\delta+1} - \bar{S}_o\langle T\rangle^{p} \tag{14}$$

and consequently

$$\frac{\partial H}{\partial\langle T_s\rangle} = p\bar{S}_o\langle T\rangle^{p-1}\left(1 - \frac{\delta+1}{p}\right) \tag{15}$$

Thus, the perturbations are stable or unstable depending upon whether $p < \delta+1$ or $p > \delta+1$ respectively, as is well-known, e.g [1,2].

Since p actually depends on T, most considered models for the thermal conductivity lead to two equilibrium solutions, one for moderate temperatures $T \gtrsim 10$ keV, which is unstable ($p \cong 2$), and another for high

temperatures $T \gtrsim 30$ keV, which is stable ($p \lesssim 1$), cf Fig. 3. However, physical and technological constraints favour the low temperature equilibrium even though this necessitates the use of active burn control methods for stabilization.

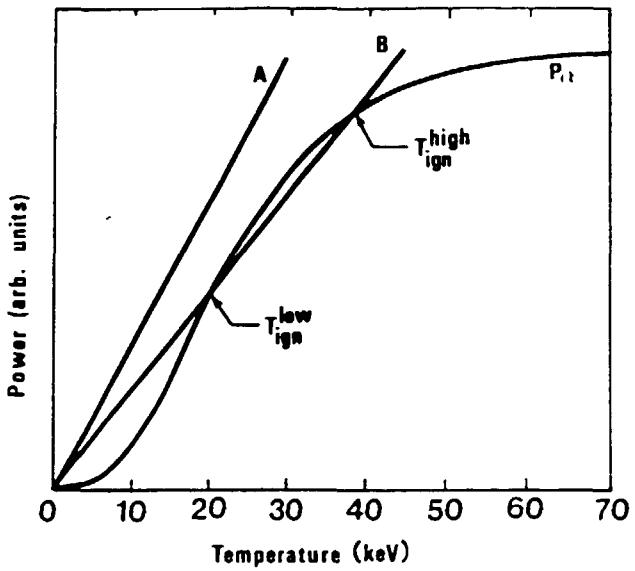

Fig. 3. Plasma heating and power loss as a function of plasma temperature with plasma power loss assumed to be linearly dependent on temperature. Two confinement scalings are denoted by A and B.

3.4. Profile analysis

In the present section we will consider in more detail the properties of eq. (3) with special emphasis on the profile characteristics of the equilibrium solutions. Introducing the normalization $x = r/a$, $y(x) = T(r)/T(0)$, and $\lambda = S_o\, T(0)^{p-\delta-1}/K_o$ the properties of the equilibrium solution are determined by the nonlinear eigenvalue problem:

$$\frac{1}{x}\frac{d}{dx}\left(xy^{\delta}\frac{dy}{dx}\right) + \lambda y^{p} = 0$$

$$y(0) = 1$$

$$y'(0) = y(1) = 0 \qquad (16)$$

where the eigenvalue, λ, determines the temperature on axis and the eigenfunction, $y(x)$, determines the radial profile of the temperature.

Exact analytical solutions of eq. (16) can only be obtained for particularly simple choices of p and δ. Although obviously eq. (16) can be solved numerically, we are here looking for simple analytical approximations which should be useful, e.g. in evaluating derived global quantities like fusion output, β-values etc.

The simplest approximate solution can be obtained by averaging eq. (16) using the weighting function $w(x) = x$. This yields for the eigenvalue

$$\lambda = \frac{4(p+\delta+1)}{(\delta+1)^2} \tag{17}$$

where again a finite loss flow at the boundary only occurs for $\alpha = 1/(\delta+1)$.

A somewhat better approximation can be expected if the physical condition of finite flow at $x = 1$ is used to determine α, i.e. the form of the eigenfunction, but a different weighting function is used for the determination of the eigenvalue, e.g. $w(x) = xy^{\delta+1}$. This implies

$$\lambda = \frac{1}{\delta+1} \frac{\int_o^1 x\left(\frac{d}{dx} y^{\delta+1}\right)^2 dx}{\int_o^1 x y^{p+\delta+1} dx} = \frac{4\left(\delta+1+\frac{p}{2}\right)}{(\delta+1)^2} \tag{18}$$

The weighting function used in eq. (18) leads to a functional form for the eigenvalue, which is reminiscent of a variational formulation. In order to use the full power of optimization of a variational approach we reformulate eq. (16) in order to allow a variational formulation. Introduce $y^{\delta+1} = z$, i.e. $y = z^{1/(\delta+1)}$. Eq. (16) can then be written as the nonlinear Sturm Liouville problem

$$\frac{1}{x}\frac{d}{dx}\left(x\frac{dz}{dx}\right)+\bar{\lambda}z^q=0$$

$$z'(0)=0=z(1) \qquad (\delta>-1)$$

$$z(0)=1 \tag{19}$$

where $q = p/(\delta+1)$ and $\bar{\lambda}=(\delta+1)\lambda$. Eq. (19) can be rewritten as the variational problem corresponding to the Lagrangian

$$L=\frac{1}{2}x\left(\frac{dz}{dx}\right)^2-\frac{\bar{\lambda}}{q+1}xz^{q+1} \tag{20}$$

Using Raleigh-Ritz optimization based on trial functions of the form $y(x) = (1-x^2)^\alpha$, it is straightforward to find the following optimal approximation:

$$\alpha=\frac{p+3(\delta+1)}{8(\delta+1)^2}\left\{1+\left[1+\frac{16(\delta+1)^2}{(p+3(\delta+1))^2}\right]^{1/2}\right\}$$

$$\lambda=4(\delta+1)\alpha^2 \tag{21}$$

The agreement between the numerical solutions and the approximations is good, especially for the variationally obtained solutions, cf. Figs. 4 and 5.

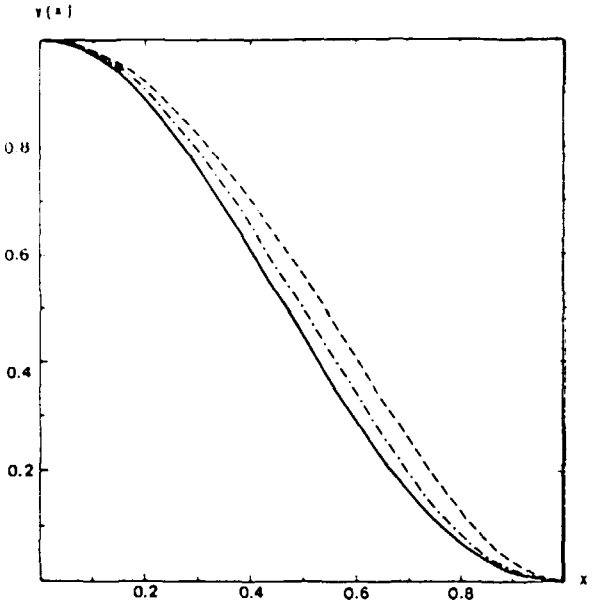

Figs 4. Comparison between numerically obtained solution (———) and approximate solutions according to $\alpha = 1/(\delta+1)$ (---) and the variationally determined α (-.-.-) respectively for the case $p = 0.5$ and $\delta = -0.5$ ($p = 1+\delta$).

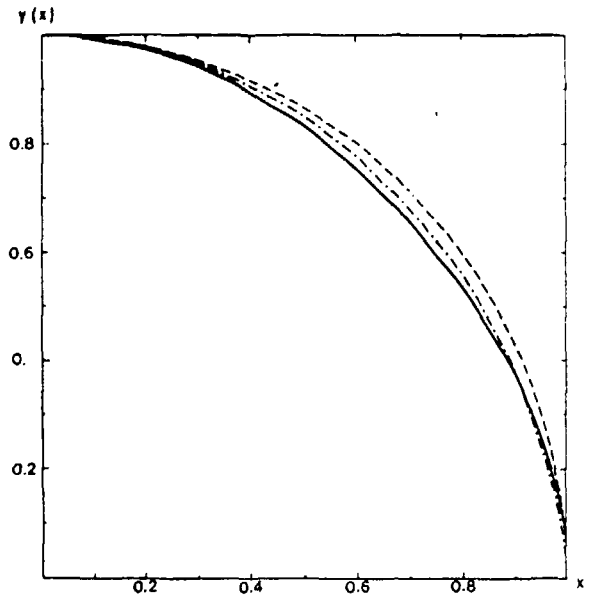

Fig. 5. Comparisons between numerically obtained solutions and approximate solutions according to $\alpha = 1/(\delta+1)$ (---) and the variationally determined α (-.-.-) respectively for $p = 1.5$ and $\delta = 1$.

Having established the properties of the stationary solution, its linear stability can be investigated by considering the linear inhomogeneous eigenvalue problem for a small perturbation of the equilibrium solution. Again, using a variational approximation for the eigenvalue, the perturba-

tions are found to be stable or unstable depending on whether $p < \delta+1$ or $p > \delta+1$ respectively, i.e. in complete agreement with the 0-D analysis. This condition is in fact equivalent to that obtained by other means, e.g. [5,6], where the profile is stable or unstable when $da/dT > 0$ or $da/dT < 0$ respectively where $a = a(T)$ is the equilibrium radius as a function of temperature on axis.

3.5. Extension to density profiles

The present approximate analysis can be generalized to include a fixed density radial profile as well as to incorporate a density dependent thermal conductivity. Thus we assume that the density is given by $n = n(0)(1-x^2)^\gamma$ and the thermal conductivity by $n\kappa/3 = k_o\, n^{\delta n} T^{\delta T}$. The energy balance equation reads

$$\frac{\partial(nT)}{\partial t} = \frac{1}{r}\frac{\partial}{\partial r}\left(r k_o n^{\delta_n} T^{\delta_T}\frac{\partial T}{\partial r}\right) + s_o n^2 T^p \qquad (22)$$

where $E_\alpha \langle\sigma v\rangle/12 = s_o T^p$. Averaging as before assuming $T(r) = T(0)(1-x^2)^\alpha$ we obtain

$$\frac{d\langle nT\rangle}{dt} = -\bar{k}_o \langle n\rangle^{\delta_n}\langle T\rangle^{\delta_T+1} + \bar{s}_o \langle n\rangle^2 \langle T\rangle^p \qquad (23)$$

where the condition of finite loss flow at $r = a$ determines the temperature profile exponent α to be $\alpha = (1-\gamma\delta_n)/(1+\delta_T)$.

and

$$\bar{k}_o = \frac{4k_o}{a^2}\frac{(1-\gamma\delta_n)}{(1+\delta_T)^{\delta_T+2}}(\gamma+1)^{\delta_n}(2+\delta_T-\gamma\delta_n)^{\delta_T+1}$$

$$\bar{s}_o = s_o \frac{(\gamma+1)^2}{p+\delta_T+1+\gamma(2+2\delta_T-p\delta_n)}\frac{(2+\delta_T-\gamma\delta_n)^p}{(\delta_T+1)^{p-1}} \qquad (24)$$

The stationary average temperature is

$$\langle T_s \rangle = \left(\frac{\bar{s}_o}{\bar{k}_o} \right)^{\frac{1}{\delta_T + 1 - p}} \tag{25}$$

The stability properties of the equilibrium are the same as before.

A profile analysis analogous to that of the previous section can also be performed. The eigenvalue, λ, which determines the temperature on axis according to $\lambda = a^2 s_o n(0)^{2-\delta n}\, T(0)^{\delta T}\, \delta_T / k_o$ is given approximately by

$$\lambda = \frac{4(1-\gamma\delta_n)^2}{(\delta_T+1)^2}\left[(\gamma+1)(\delta_T+1) + \frac{p}{2}(1-\gamma\delta_n) \right] \tag{26}$$

3.6 Application

As an illustration of the application of the present analysis we will consider a thermonuclear plasma satisfying the INTOR scaling for the thermal conductivity, viz.

$$n\kappa \equiv 5 \cdot 10^{17}\ \mathrm{cm^{-1}s^{-1}} \tag{27}$$

We will furthermore assume $n(r) = n(0)(1-r^2/a^2)$, $n(0) = 2 \cdot 10^{14}\ \mathrm{cm^{-3}}$ and $a = 150$ cm. In the temperature range $10 \leq T$ keV we approximate, cf Figs. 1 and 2, $\langle \sigma v \rangle \equiv 6 \cdot 10^{-19}\, T^{2.2}\ \mathrm{cm^3 s^{-1}}$ where T is in keV. The characteristic profile factors are $\delta_n = \delta_T = 0$, $\gamma = 1$, $p = 2.2$ which implies that $\alpha = 1$ and from eq. (26) $\lambda = 12.4$. The peak temperature T(0) is found to be $T(0) \cong 9$ keV in acceptable agreement with the result of Ref. [5].

Summary

The present analysis has considered the equilibrium and stability properties of the power balance equation determining the temperature evolution in a burning fusion plasma. Special emphasis has been given to a consistent profile averaging of the radial transport equation to obtain a simplified zero dimensional model equation, the determination of approximate solutions for the equilibrium temperature profiles, as well as the stability properties of the corresponding 0-D and 1-D equations. For a more detailed presentation of the analysis, see [8]. Although the results of the stability analysis are well-known, the method of approach gives some new insight into the thermal runaway problem and in particular the relation between 0-D and 1-D models. The extension of 0-D models to allow for a more complete description involving radial transport models is presently attracting considerable attention, [2,9].

References

[1] K. Borrass, Physica Scripta T16 (1987), 107.

[2] G.T. Sager, Tokamak Burn Control, internal report, Fusion Studies Laboratory, University of Illinois, Urbana, Illinois, USA (1988).

[3] S.V. Putvinski, Sov. J. Plasma Physics, 6 (1981), 694.

[4] M. Becker, The Principles and Applications of Variational Methods, MIT Research Monograph No. 27 (1964).

[5] Ya.I. Kolesnichenko, S.N. Reznik, and V.A. Yavorski, Nucl. Fus. 16 (1976), 105.

[6] Ya. I. Kolesnichenko, Nucl. Fus. 20 (1980), 727.

[7] Ya. I. Kolesnichenko, V.V. Lutsenko, S.N. Reznik, internal report, Kiev Institute for Nuclear Research (1987).

[8] D. Anderson, H. Hamnén and M. Lisak, CTH-IEFT/PP-1989-19.

[9] S.W. Haney, ITER Burn Control Workshop, December 16 (1988), Lawrence Livermore Nat. Laboratory.

4. SOME EMERGING THOUGHTS ON BURN CONTROL

4.1 On the maximum Q in subignited operation

The stabilization of thermal runaway can be obtained by working in the subignition regime (nearly ignited plasma), with actively controlled time-varying auxiliary heating. Symbolically, the evolution of a perturbation δT around an equilibrium temperature T_o can be written as:

$$3n \frac{d}{dt}(\delta T) = P_\alpha(T_o + \delta T) + P_{aux}(T_o + \delta T) - \frac{3nT}{\tau_E}\Big|_{T_o+\delta T} \qquad (1)$$

where P_{aux} denotes the auxiliary heating power, assumed to be controlled by some feedback function. Since T_o is assumed to be an equilibrium point,

$$P_\alpha(T_o) + P_{aux}(T_o) - \frac{3nT}{\tau_E}\Big|_{T_o} = 0 \qquad (2)$$

In Eq. (1), the maximum allowable negative perturbation is determined by the available heating power, $P_{aux} < P_{max}$. The maximum positive perturbation follows from the requirement $P_{aux} > 0$.

Conversely, the equilibrium point T_o together with a specification o the maximum allowed positive perturbation δT_{max} determines the necessary equilibrium heating power, P_{aux} (T_o), or in other words the maximum Q-value for control to be possible.

The problem of finding Q_{max} as a function of T_o and δT_{max} was analyzed in Ref. [1], using a two-fluid, 1-D, model for electrons and ions. Neoclassical thermal conductivity was assumed for the ions and a constant conductivity corresponding to the scaling law

$$\tau_e = 1.9 \cdot 10^{-21}\, n_o a^2$$

was taken for the electrons. Both centrally peaked and edge peaked auxiliary heating profiles, deposited either on ions or on electrons, were studied. A typical result from [1], showing Q_{max} as a function of the central equilibrium ion temperature, for different values of allowable perturbation, is shown in Fig. (1).

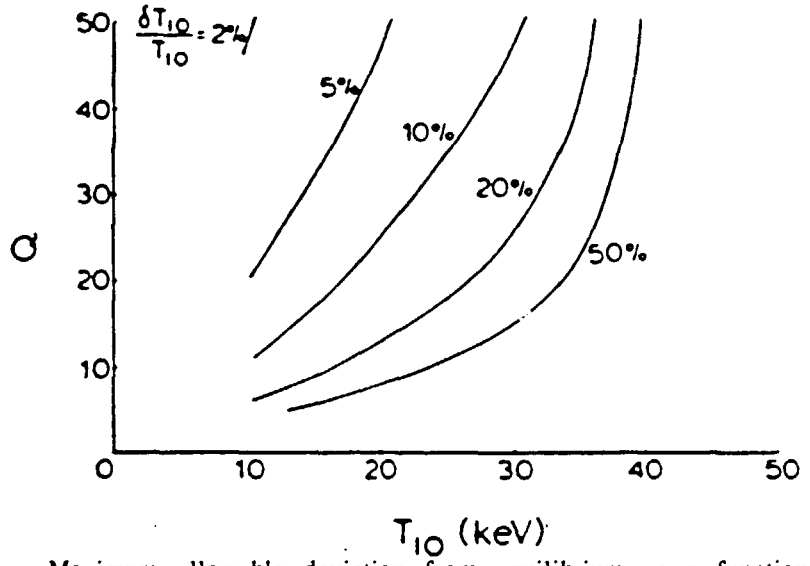

Fig. 1. Maximum allowable deviation from equilibrium as a function of the central ion temperature and the power multiplication factor Q for centrally peaked auxiliary heating of the ions. (From [1]).

We note here that the essential features contained in the results of Ref. [1] can be obtained qualitatively without much involved analysis. Namely, as noted above, using that the maximum positive temperature perturbation is when the auxiliary heating must be completely shut off in order not to have a growth of the temperature, i.e.

$$0 = \langle 3n \frac{d}{dt} (\delta T) \rangle = \langle P_\alpha (T_o + \delta T_{max}) \rangle - \frac{\langle 3nT \rangle}{\tau_E} \Big|_{T_o + \delta T_{max}} \qquad (3)$$

where we have also applied a volume average, we find by a Taylor expansion of the RHS. and using Eq. (2), omitting for brevity the angular brackets:

$$P_{aux}(T_o) \equiv \delta T_{max} \cdot \frac{\partial}{\partial T}\left(P_\alpha - \frac{3nT}{\tau_E}\right)_{|T=T_o}$$

yielding

$$Q_{max} \equiv \frac{5P_\alpha}{P_{aux}}\,|_{T=T_o} \equiv \left[\frac{\varepsilon T_o}{5P_\alpha}\frac{\partial}{\partial T}\left(P_\alpha - \frac{3nT}{\tau_E}\right)\right]^{-1}_{T=T_o} \tag{4}$$

where

$$\varepsilon = \frac{\delta T_{max}}{T_o} \tag{5}$$

From Eq. (4) we find

$$Q_{max} \equiv \frac{5}{\varepsilon}\,\frac{1}{p-1-\delta} \tag{6}$$

where we have assumed Q >> 1 and where as before (cf Sec. 3)

$$p(T_o) = \frac{\partial \ln \langle\sigma v\rangle}{\partial \ln T}\,|_{T=T_o} \tag{7}$$

and δ is the scaling exponent of the thermal conductivity with temperature. We also find that the thermal runaway time, defined from

$$\frac{\partial(T-T_o)}{\partial t} = \frac{T-T_o}{\tau_{runaway}} \tag{8}$$

can be written as

$$\tau_{runaway} \equiv \frac{\tau_E}{p-1-\delta} \tag{9}$$

Eq. (6) shows a reasonable agreement with the results of Ref. [1]. The equilibrium temperature T_0 should be regarded as the volume averaged temperature. Using the approximate relation (c.f. Sec. 3)

$$\hat{T} = \frac{\delta+2}{\delta+1} \cdot T_o \qquad (10)$$

for the central temperature, Eq. (6) is plotted in Figs. (2a-c) for three different choices of δ; δ = 0.5, 0; + 0.5. As can be seen, the achievable Q_{max} depends strongly on δ. Taking as an example the maximum relative perturbation to be ε = 0.2 (which could prove difficult to improve upon because of diagnostic uncertainties among other things, c.f. also Sec. 4.3), we find with δ = 0 and T = 20 keV, Q_{max} ~ 10-15. Such a figure, obviously, would be inconveniently low from a reactor point of view.

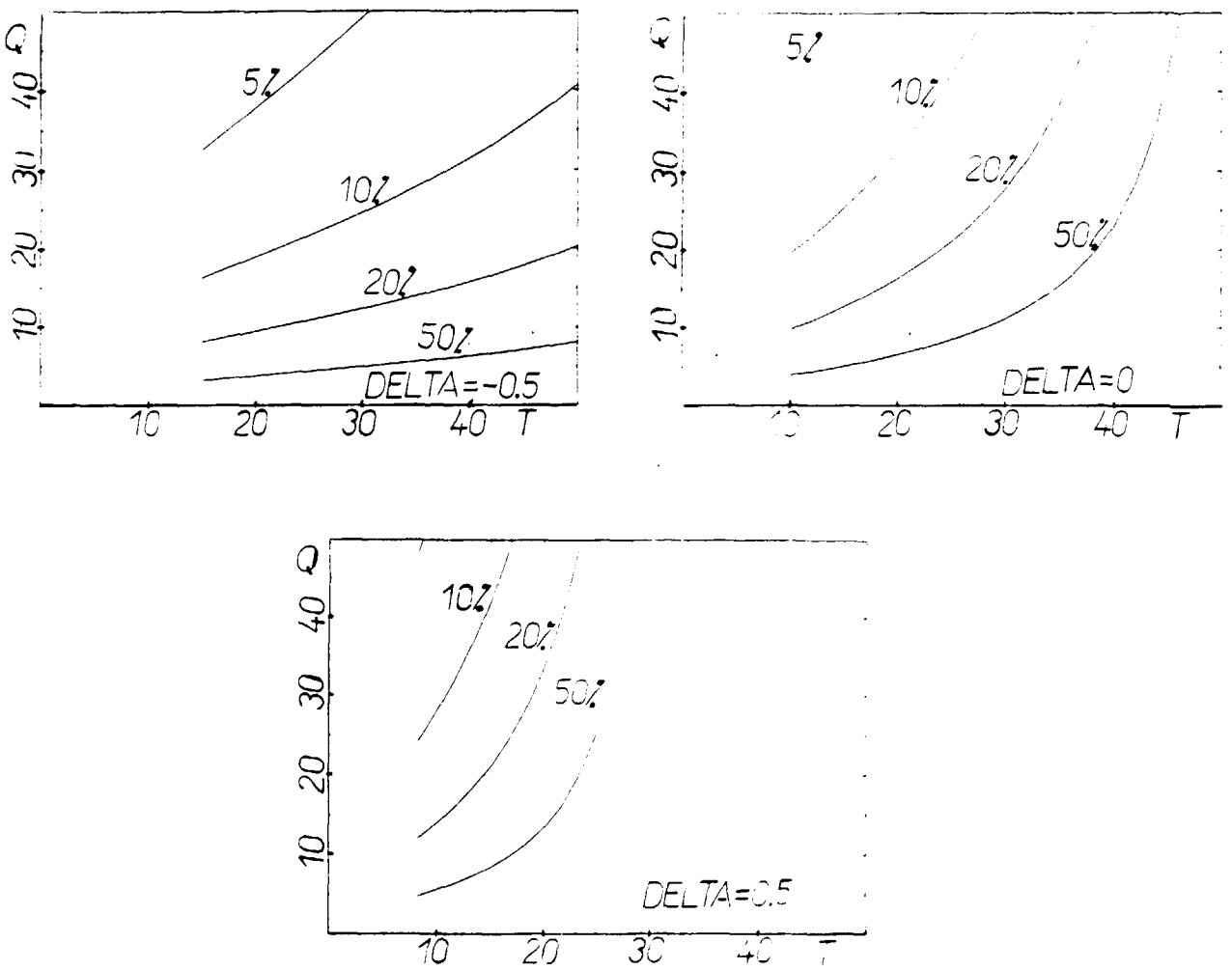

Fig. 2. Q_{max} as a function of central ion temperature for different allowable temperature deviations and for different temperature scalings, δ, of the thermal conductivity a) δ = -0.5 b) δ = 0 and c) δ = 0.5

4.2 Conditions for the initial development of the temperature

Assuming that the temperature profile corresponding to equilibrium of a chosen operating point is known, we are faced with the following problem: Suppose that the instantaneous measured profile is different from the equilibrium profile, e.g. that it is hotter near the centre and colder near the edge. What will the subsequent evolution be? Will the plasma self-heat to high temperatures or will the burn be quenched? Could a simple criterion be given to separate the two cases? The answer to this question obviously determines which control action to take, e.g. whether to increase the auxiliary heating or let the plasma self-heat. To see that the question is non-trivial, consider Figs. (3a, b), which are results of a numerical study of the dynamics of a model equation for burn stability, given below. The graphs show the evolution of two profiles, initially with the same profile shape, but with slightly different axial values. As can be seen, for both cases the axial temperature initially decreases, but at later times one case self-heats and the other is quenched. Thus, the need for a sophisticated control criterion is obvious. E.g. the momentaneous change in axial temperature is not sufficient in this situation, but instead some sort of integral criterion is needed.

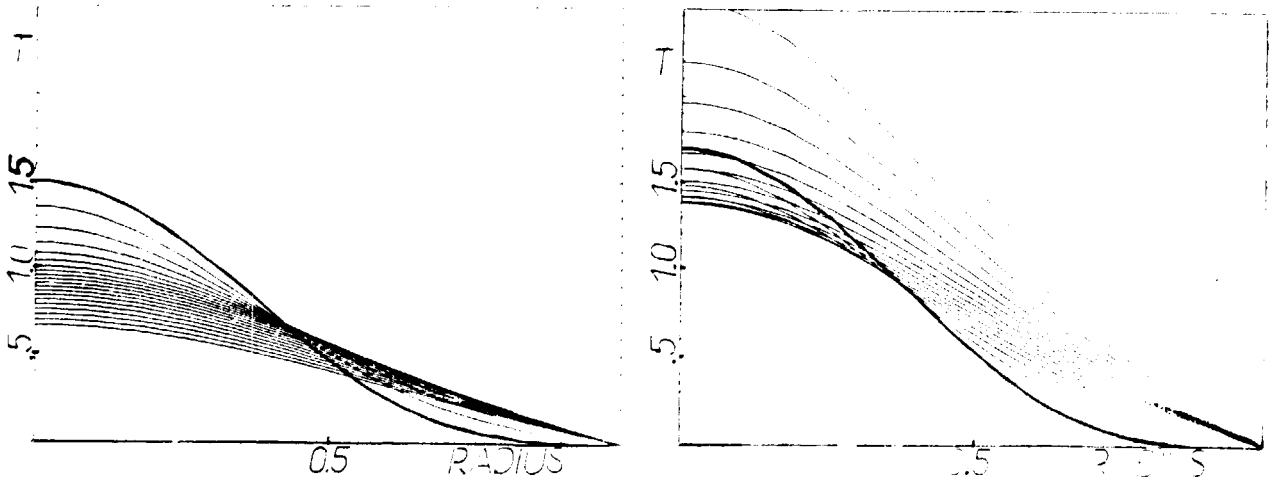

Fig. 3. Time evolution of two temperature profiles initially with the same profile shape (solid line), but with slightly different axial values. In both cases the central temperature decays initially, but in the case to the right it later recovers and ends up in runaway.

Therefore, work has started in order to try to find such a suitable criterion. The model equation studied is given by

$$\frac{\partial T}{\partial t} = \frac{1}{x}\frac{\partial}{\partial x}\left(xT^{\delta}\frac{\partial T}{\partial x}\right) + \lambda T^{p} \tag{10}$$

(c.f. Sec. 3), with initial and boundary conditions

$$\begin{aligned} &T(x,0) = T_o(1-x^2)^{\gamma} \\ &T'(0,t) = 0 \\ &T(1,t) = 0 \end{aligned} \tag{11}$$

The same normalization as in Sec. 3 has been used so that λ is taken as

$$\lambda = \frac{4(\delta+1+p/2)}{(\delta+1)^2} \tag{12}$$

In accordance with Sec. 3, we expect the equilibrium solution of (10) to closely resemble

$$T_{eq} \equiv (1-x^2)^{1/1+\delta} \tag{13}$$

Problems similar to this one has been studied before, see, e.g. [2,3]. In Ref. [2], it was suggested that regions of runaway and quench could be separated by

$$\int_o^1 T(x,0)xdx \gtrless \alpha \int_o^1 T_{eq}(x)\,xdx \tag{14}$$

where the coefficient α depends somewhat on the exact profile shapes, though always being of the order unity. In other words, thermal runaway is determined by whether or not the momentaneous thermal (energy) content is more or less than the equilibrium content. Using the results of Sec. 3, we have

$$W_{eq} \equiv \int_o^1 T_{eq}(x)\, x dx \cong \frac{1}{2}\,\frac{1+\delta}{2+\delta} \tag{15}$$

So far, we have primarily been studying the dynamics of profiles which are initially more peaked than the equilibrium profile (13). The preliminary conclusion is that the criterion (14) tends to overestimate the thermal content needed to get runaway. However, for the numerical solution of Eq. (10), a rather crude explicit scheme has been used, so that the quantitative statements may have to be reexamined.

To examine the stability of the assumed equilibrium solution we first illustrate the case $\gamma = 1/(1+\delta)$, $p = 2$, $\delta = 0$ ($\lambda = 8$). Shown in Fig. (4) is the time evolution of the thermal content

$$W(t) = \int_o^1 T(x,t)\, x dx \tag{16}$$

for different initial T_o. In Figs. (5a, b) are shown the corresponding evolution of profiles.

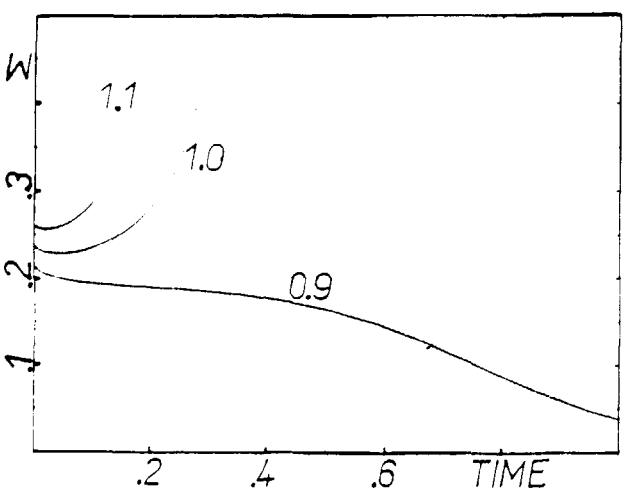

Fig. 4. Time evolution of the thermal content for initial peaking factor $\gamma = 1/(1+\delta)$, $p = 2$, $\delta = 0$, for three values of initial axial temperature $T_o = 0.9, 1.0; 1.1$.

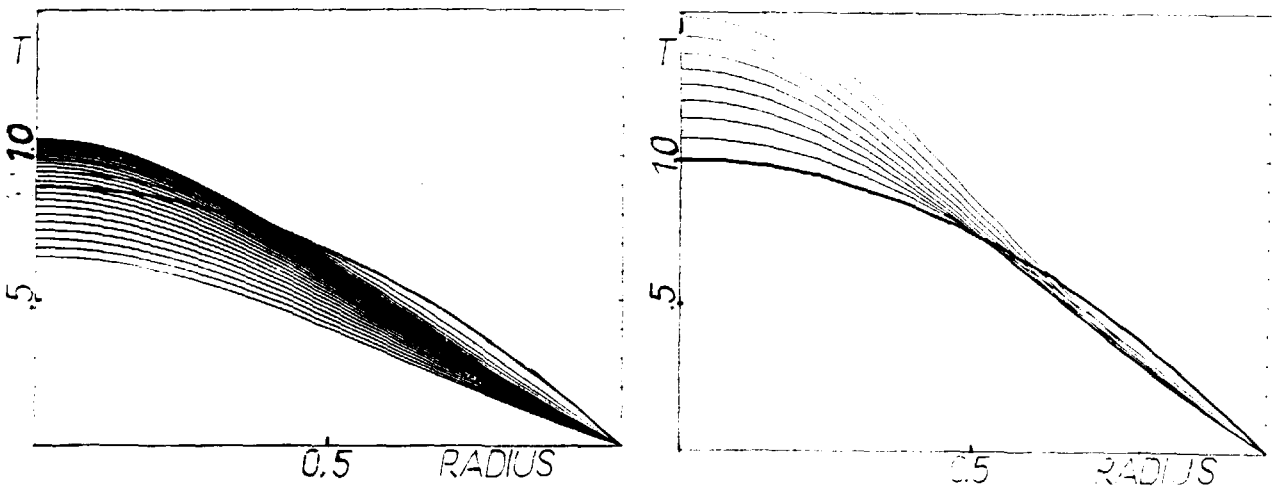

Fig. 5. Time evolution of temperature profile with the same parameters as for Fig. 4, a) $T_0 = 0.9$ b) $T_0 = 1.0$. Solid lines mark the initial profiles.

It appears that the approximation for the equilibrium profile is reasonable, although it seems to predict slightly too broad profiles.

It is intuitively clear that for a highly peaked initial profile, the time evolution will consist of two phases. A first fast phase, where by heat conduction the central peak will spread out, so that the resulting profile will be similar in shape to the equilibrium profile. Thereafter follows a phase of either runaway or quenching with essentially fixed profile shape. It is then also clear that the separation between runaway or quench is determined by whether or not the profile lies above or below the equilibrium profile by the end of the first phase. A criterion like Eq. (14), with $\alpha = 1$, says just this. However, it neglects the change in thermal content during the first phase. In order to include this, we have tried Taylor expanding the thermal content, and thus write the criterion for thermal runaway as

$$W_{eq} - W(\tau) \cong W_{eq} - W(0) - \dot{W}(0)\cdot\tau - \ddot{W}(0)\cdot\frac{\tau^2}{2} < 0 \qquad (17)$$

where τ is a measure of the length of the first phase and where $\dot{W}(0)$ and $\ddot{W}(0)$ are numerically calculated here but corresponds to quantities which are semi-momentaneously measurable. To find an estimate of the time-scaie τ, we note that close to the axis, a generalized parabola can be fitted by a Bessel function:

$$(1 - x^2)^{\alpha} \equiv J_0(2\sqrt{\alpha} \cdot x), \quad x << 1 \qquad (18)$$

For a highly peaked profile, the presence of the boundary at x = 1 should initially not play an important role. Thus, from the solution to the free expansion problem with initial profile as in Eq. (18) we find a measure of the characteristic time constant for decay

$$\tau = \frac{1}{(2\sqrt{\alpha})^2} = \frac{1}{4\gamma} \qquad (19)$$

In Fig. (6) we compare the criteria (14) with α = 1 and (17) with the numerically derived boundary between cases resulting in runaway and quenching. Although the prediction given by Eq. (17) is not perfect, it seems to be a step in the right direction and further studies may improve the situation

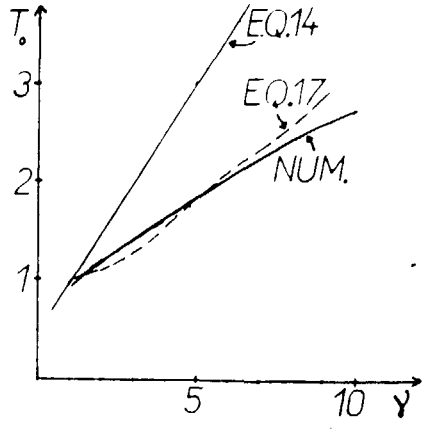

Fig. 6. Comparison of analytically and numerically derived criteria for the separation of cases resulting in runaway on quench. The case shown is for the parameter choice p = 2, δ = 0 and gives as a function of initial peaking factor γ the necessary initial axis temperature.

4.3 Some implications of sawtooth activity for burn control

A prominent feature in modern Tokamak experiments is the presence of significant sawtooth activity. The characteristic sawtooth variation in time has been observed in electron and ion temperatures as well as in plasma density but also in signals relating to fusion produced quantities like neutron and high energy charged particle emission. Although an effort is made to conceive methods for suppressing the sawteeth, it seems likely that sawtooth oscillations will be present also in Tokamaks operating near or under ignition conditions. In fact, it has even been suggested that the suppression and excitation of sawtooth oscillations might be used to modify plasma energy confinement and thereby to act as a burn control method. However, making the conservative assumption that sawteeth do not easily lend themselves to be controlled, one should examine their effects on burn control. In particular, the presence of sawteeth complicates the active feedback control of an unstable equilibrium temperature profile. Two aspects of this problem will be tentatively discussed: (i) the profile changes involved in the sawtooth process complicates the interpretation of neutron emission signals if these are used to infer central ion temperatures and (ii) the sawtooth temperature variation implies an inherent Q-limitation for subignited scenarii.

Neutron yield variation in sawtooth dominated plasmas

Assuming $\langle\sigma v\rangle \sim T^p$ the volume averaged neutron yield, S, becomes

$$S \propto \int n^2 T^p \, dv \qquad (20)$$

The ion density and temperature profiles are modelled according to $n(r) = n(0)(1-r^2/a^2)^{\alpha}$ $T(r) = T(0)(1-r^2/a^2)^{\beta}$. The relative change of the neutron yield during a sawtooth event is,

$$\frac{\Delta S}{S} = 2\,\frac{\Delta n(0)}{n(0)} + p\,\frac{\Delta T(0)}{T(0)} - \frac{2\Delta\alpha + p\Delta\beta}{2\alpha + p\beta + 1} \qquad (21)$$

where the last term accounts for the effect of the changing density and temperature profiles during the sawtooth. Indeed, the last term in general significantly affect the neutron yield and must be taken into account in order to relate correctly the variations of neutron emission and temperature, [4].

Using the assumption that the total ion particle and energy densities in the plasma remain constant during a sawtooth crash eq. (21) can be rewritten, [4]

$$\frac{\Delta S}{S} = \frac{2\alpha + p\beta}{(2\alpha + p\beta + 1)[1 + K(\alpha)(\alpha + 1)]}\,\frac{\Delta N}{N} +$$

$$+ \frac{p[\alpha + (p-1)\beta]}{2\alpha + p\beta + 1}\,\frac{\Delta T(0)}{T(0)} \qquad (22)$$

where $K(\alpha)$ can be expressed in terms of the logarithmic derivative $\psi(x)$ of the Gamma function according to

$$K(\alpha) = \psi(\alpha + 1) - \psi(\alpha + 3/2) \qquad (23)$$

and N and ΔN denote central line integrated density and the corresponding variation respectively. Generally the contribution coming from the density variation is significantly smaller than that coming from the temperature variation. Neglecting the former contribution we have

$$\frac{\Delta S}{S} \cong \frac{p[\alpha + (p-1)\beta]}{2\alpha + p\beta + 1}\,\frac{\Delta T(0)}{T(0)} \qquad (24)$$

as compared to the relation

$$\frac{\Delta S}{S} \cong p\,\frac{\Delta T(0)}{T(0)} \qquad (25)$$

which is obtained if profile effects are neglected. Assuming parabolic density profile ($\alpha = 1$) and taking a temperature profile consistent with a thermal conductivity scaling $\kappa \sim T^{\delta}$, i.e. $\beta = 1/(1+\delta)$ we obtain from eq. (22), using $p \equiv 2$:

$$\frac{\Delta S}{S} \cong \frac{4+2\delta}{5+3\delta}\,\frac{\Delta T(0)}{T(0)} \tag{26}$$

e.g. for $\delta = 0$, $\Delta S/S \sim 0.8\ \Delta T(0)/T(0)$, as compared to $\Delta S/S = 2\ \Delta T(0)/T(0)$ according to eq. (25). Thus, we conclude that changing profiles in connection with sawtooth activity in burning plasmas is an important effect to be considered when neutron diagnostics are to be used for feedback control of unstable equilibria.

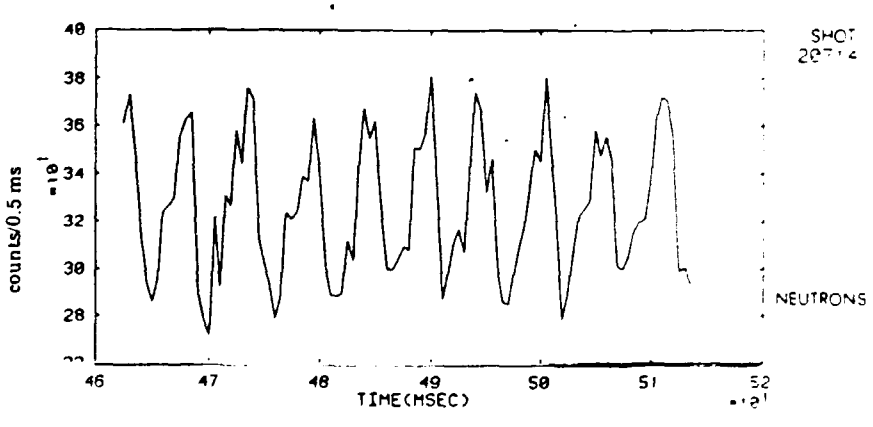

Fig. 7a. Time evolution of the total neutron flux in FT sawtooth discharges, [4].

Fig. 7b. Time evolution of the total neutron flux averaged over 17 subsequent sawteeth during the current flat top, [4].

Sawtooth induced Q-limitations of subignited operation

The presence of sawtooth activity in a fusion plasma should be particularly complicating for a feedback controlled subignited plasma since such a plasma should work as close as possible to the ignition temperature in order to achieve high Q-values. This implies that especially positive temperature excursions from the operating temperature are particularly dangerous since the control measure is passive, i.e. decreasing the auxiliary heating. Thus, the maximum positive temperature excursion is determined by $P_{aux} = 0$.

Furthermore, the control system must be "intelligent" enough to distinguish between the inherent sawtooth excursions and real thermal runaway. This may, in fact, prove exceedingly difficult partly because the characteristic sawtooth period can be expected to be of the same order as the thermal runaway time and partly because the sawtooth period may vary on the same machine. On, e.g. JET the sawtooth period can vary from ~ 100 ms up to monster sawteeth extending over several seconds. In addition the magnitude of the sawtooth may also vary significantly. This is illustrated in Figs. (8-10).

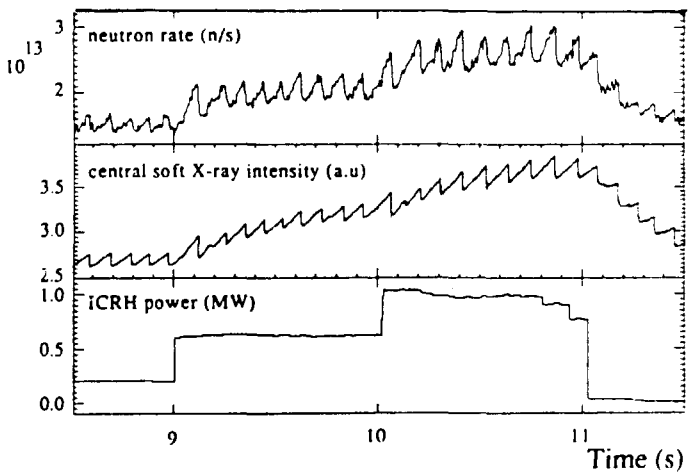

Fig. 8. Time dependence of 2.5 MeV neutrons, soft x-rays from the plasma centre and ICRH power for a typical ^{3}He minority heated discharge in JET, [5].

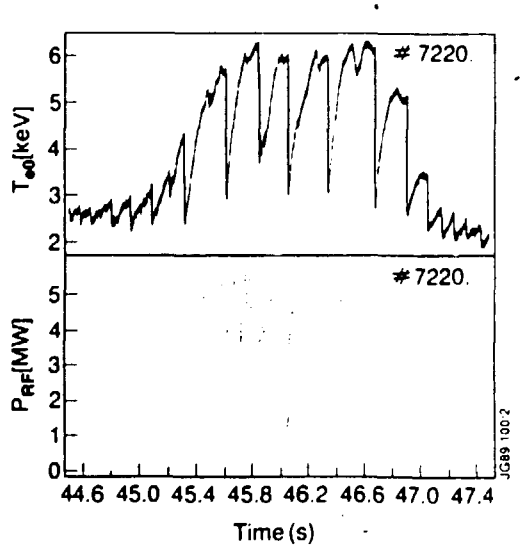

Fig. 9. The giant sawteeth activity in JET with increased amplitude and period of sawteeth during ICRH (I_p = 2 MA, q_ψ = 6), [6].

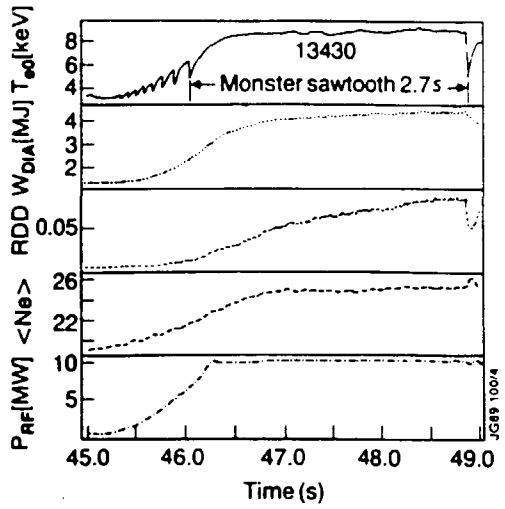

Fig. 10. A characteristic "monster" sawtooth JET discharge with sawtooth stabilization by minority ICRF heating, [6].

If the sawtooth activity is accepted as part of normal operation, at least a 20% inherent variation in peak temperature must be allowed for. To this must be added the uncertainty of the measurement which may add another 20% (conservative estimate). This implies that the operating temperature must lie at least 20-30% below the ignition temperature and that the maximum achievable Q is approximately 10-15 as discussed in section 4.1.

Thus we conclude that sawtooth activity should be a problem of great concern for high-Q subignited operation of fusion reactor plasmas.

4.4 Thoughts on alternative control actions

As noted previously, a large number of schemes have been proposed in order to control the thermonuclear burn at an unstable operating point. However, most of these have drawbacks associated with them, e.g. in terms of power consumption or compatibility with reactor design or simply because the physics of the proposed mechanism is poorly understood. Therefore, there seems to be a need to invent alternative methods, in the hope of eventually finding a more suitable scheme. We have tried also to

think along these lines and below we present two embryos for ideas in this direction, one of which does not appear effective and one which may be worth pursuing.

Control by variation of effective minor radius

As shown in Sec. 3, the average temperature in equilibrium is related to minor radius according to

$$<T_s> = \left(\frac{\bar{S}_o}{\bar{K}_o} \right)^{\frac{1}{\delta+1-p}} \approx a^{2/\delta+1-p} \qquad (27)$$

Thus, e.g. for the case p = 2, δ = 0.5, we see that a 5% change in minor radius a is sufficient to produce a 20% change in $<T_s>$. Hence, if a suitable method of changing the effective plasma radius could be devised, then this may be a practical method for control. One method of doing this could perhaps be to move the divertor x-point in and out, if e.g. this is possible on the required timescale and if the resulting changes in deposition profile on the divertor plates would be tolerable. Another method may be to strongly increase the heat conductivity in the outer regions of the plasma, thereby effectively reducing its size. This may prove possible to accomplish if turbulence could be induced by injected edge-localized waves or if time varying magnetic field ripple could be introduced in the outer plasma by external windings.

Dynamic stabilization

It is well-known in mechanics that an unstable equilibrium point may be stabilised if a suitable periodic force is applied. For example, the unstable equilibrium of an inverted pendulum can be stabilized if its base point is forced to perform an updown motion with an amplitude and frequency in a certain range. Also in plasma physics, dynamic stabilization has been

proposed for stabilization of e.g. the Rayleigh-Taylor instability, see e.g. the review [7].

We have briefly examined whether the same technique could be applied for burn control. It has been assumed that sinusoidally modulated auxiliary heating is applied to the plasma, giving the energy balance equation

$$3n \frac{dT}{dt} = F(T) + P_o \cos\omega t \tag{28}$$

where

$$F(T) = P_\alpha(T) - \frac{3nT}{\tau_E} + \bar{P}_{aux} \tag{29}$$

with $\bar{P}_{aux}$ being the time averaged auxiliary heating power. Suppose that $T = T_o$ is an unstable equilibrium solution of (28) with $P_o = 0$, i.e. that

$$F(T_o) = 0$$

$$\frac{\partial F}{\partial T} \Big|_{T=T_o} > 0 \tag{30}$$

Introducing $\delta T = T - T_o$ we find by Taylor expanding around the equilibrium point

$$3n \frac{d(\delta T)}{dt} = \delta T \cdot \frac{\partial F}{\partial T} \Big|_{T=T_o} + \frac{(\delta T)^2}{2} \cdot \frac{\partial^2 F}{\partial T^2} \Big|_{T=T_o} + P_o \cos\omega t \tag{31}$$

To simplify the notation, we have studied the model equation

$$\frac{dy}{dt} = ay + by^2 + \cos\omega t \tag{32}$$

where $a > 0$. Eq. (32) is a special case of the generalized Riccati equation:

$$\dot{y} = f(t) + g(t)y + h(t)y^2 \tag{33}$$

which is known to have the general solution

$$y(t) = -\frac{1}{h(t)} \cdot \frac{C\dot{u}_1 + \dot{u}_2}{Cu_1 + u_2} \tag{34}$$

where C is a constant to be determined by the initial condition, and u_1 and u_2 are linearly independent solutions of the equation

$$\ddot{u} + P(t)\dot{u} + Q(t)u = 0$$

$$P(t) = -\left(g + \frac{\dot{h}}{h}\right) = a$$

$$Q(t) = bc \cdot \cos\omega t \tag{35}$$

With the transformation

$$u(t) = v(t) \cdot w(t)$$

$$w(t) = e^{-\int P/2\, dt} = e^{-a/2 \cdot t} \tag{36}$$

we find

$$\ddot{v} + (\alpha + \beta \cos\omega t)v = 0$$

$$\alpha = -\frac{a^2}{4}$$

$$\beta = b \cdot c \tag{37}$$

This is the Mathieu equation and is formally identical to the equation resulting in the case of the inverted pendulum. Hence there exists ranges

for the parameters for which the general solution of (37) is stable and oscillatory. However, for the solution (34) of the original problem

$$y(t) = -\frac{1}{b}\frac{\frac{d}{dt}[(Cv_1 + v_2)\cdot w]}{(Cv_1+v_2)w} \tag{38}$$

where v_1 and v_2 are the independent solutions of the Mathieu equation, we see that these oscillatory solutions would correspond to instability for the Riccati equation, in that whenever $Cv_1 + v_2 = 0$, $y(t)$ diverges.

Thus, it appears likely that dynamic stabilization of the burn instability could not be achieved in this way. However, the remaining possibility of utilizing parameter ranges where the solution of the Mathieu equation does not pass through zero should be further investigated before a definite conclusion could be reached.

References

[1] Bromberg, L., Fisher, J.L., Cohn, D.R., Nucl. Fus. 20(1980), 203.

[2] Kolesnichenko, Ya.I., Lutsenko, V.V., Reznik, S.N., "Alpha Particle Physics and Thermonuclear Burn in Tokamaks", USSR-US Workshop "Experimental Systems with Ignition Including the OTR and TIBER Plans", Leningrad (July 1987).

[3] Arinichev, A.D., Zhogolev, V.E., Putvinskii, S.V., Chuyanov, V.A., Sov. J. Plasma Phys. 12(1986), 835.

[4] Batistoni, P., Rapisarda, M. and Anderson, D., Measurement and Analysis of Neutron Sawteeth on FT, Nucl. Fus. (to appear).

[5] Sadler, G., Conroy, S., Jarvis, O.N., van Belle, P., Adams, J.M., and Hone, M., Investigations of Fast Particle Behaviour in JET Plasmas using Nuclear Techniques, Alpha Particles in Fusion Research, Kiev, October 23-26, 1989.

[6] Bhatnagar, V.P., Taroni, A., Ellis, J.J., Jacquinot, J., and Start, D.F.H., ICRF Power-Deposition Profiles, Heating and Confinement of Monster-Sawteeth and Peaked-Density Profile Discharges in JET, JET-P(89)38.

[7] Berge, G., Nucl. Fus. 12(1972) 99.

5. Requirements on diagnostics

For the purpose of controlling the plasma with respect to burn conditions one will require information about plasma quantities of relevance for the control process like the fuel concentration, fuel composition (i.e. n_D/n_T, fuel temperature, alpha particle heating, additional heating power, β- and Q-values. All quantities have to be known as functions of time. Quantities directly involved in the burning process, like densities, temperatures and alpha particle heating power density have to be known also as functions of radius.

5.1 Accuracy and time resolution

Whenever a deviation from the working point occurs in a burning plasma some sort of control action has to take place in order to bring the parameter values back to the desired values. Regardless of the method chosen some distortion of the fuel ion distribution has to be the result, whether it is caused by direct heating or cooling of the ions or indirectly through a density modification. In any case for a large modification of the fuel energy distribution the interpretation of the fuel temperature measurement becomes more difficult as opposed to a minor modification.

As an example we consider an ITER plasma with a 15 keV central temperature and central density equal to $4 \cdot 10^{20}\,m^{-3}$ (and $n_D/n_T = 0.5$), profile peaking factor (for parabolic profiles) equal to 4, and 100 MW neutral deuterium beam heating. Calculations of the fractional neutron sources, i.e. thermal-thermal, beam-thermal and beam-beam reactions give the ratios 0.9/0.09/0.01. Thus in this case the evolution of the ion temperature through measurements of neutron energy spectra would just be possible. The power level referred to in this case represents the full neutral beam power capable of bringing the plasma from low temperature and low density conditions to full power (1000 MW) performance in a time period of a few seconds.

As a control reference case we consider a situation when the total energy content decreases by 10 per cent within a time interval of 0.1 s. Regardless whether this is due to a loss of fuel density or a decrease in ion temperature or a combination of both, the decrease will be reflected in a 20 per cent decrease in neutron production and consequently in a 20 per cent decrease in alpha particle heating power (i.e. ~ 40 MW). To compensate for this the additional power needed for heating the plasma would be of the same order. Thus for this particular case the neutron spectra would contain approximately 4 per cent of beam-thermal neutrons and consequently the ion temperature measurements through evaluation of neutron spectra or by any other diagnostic technique would be relatively reliable because the distortion of the fuel energy distribution is negligible.

To measure a variation of 10 per cent in total neutron emission within a time period of 0.1 s is a relatively straightforward matter. To measure the fuel ion temperature within the same time period is feasible although it would require sofisticated instruments and a fast evaluation procedure. Evaluation of fuel concentration either from neutron measurements or from measurements of line radiation of impurities is a tedious work and requires a lot of considerations before it can be made on line. For improvement of evaluation of measured data further research and development work is needed.

One complication which occurs on timescales around 0.1 s is interference of sawtooth oscillati ns which could easily cause variations in neutron emission exceeding the 10 per cent level.

In case one does not want the control system to act upon such oscillations it is not at the moment obvious how a distinction of these oscillations from ordinary global energy losses can be made. One possible way might be to use the time derivative of the neutron emission signal. E.g. in JET this has a much faster decay time (~ 50-100 ms) than signals caused by global

energy losses with fall times approximately equal to 500 ms. The whole issue concerning the treatment and interpretation of global neutron emission signal has to be further investigated.

5.2 Profile measurements

The demands on the spatial resolution of the neutron emission measurement is related to the level of accuracy in the measurements and the profile of the neutron source. If we again require a 10 per cent accuracy in emissivity measurements the spatial resolution must correspond to a smaller distance than does a 10 per cent variation in neutron emissivity along the minor radius. With peaking factors (for a parabolic neutron source profile) ranging from 5 to 12 (obtained from JET data) this distance is approximately equal to 10 cm in the ITER geometry.

5.3 Summary of diagnostics requirements

In conclusion one needs to achieve qualities in measured or evaluated plasma parameter values used in the algorithm for burn control as given in Table 1. Some diagnostic techniques used in todays tokamaks allow for measurements according to the requirements. However, for some evaluated values like n_f and T_f the experience of today is limited and further research and development work will be needed.

Table 1.

Evaluated or measured quantity	Accuracy (%)	Time resol. (s)	Spatial resol. (cm)
T_f (r,t)	10	0.1	10
T_e (r,t)	10	0.1	10
n_D (r,t)	10	0.1	10
n_T (r,t)	10	0.1	10
P_α (r,t)	10	0.1	10
β	10	0.1	-
Q	10	0.1	-

6. Process identification

6.1 Description

Process identification is an analysis technique which allows to determine the dynamics of complex processes. It is based on real measurements of a set of physical signals which represent the process to be evaluated.

Process identification is today broadly applied in various fields like nuclear power reactor technology, chemical process technology, geophysics, aeronautics, biological research and speech processing to name a few.

Our experience comprises both code development work as well as practical applications mainly at the Swedish nuclear power plants during the last two decades.

Some applications to fusion have recently been developed and tested at JET. They concern the control of plasma density, vertical and radial plasma positioning and detection of leakage in a cooling system for magnets.

Simplified the method can be explained as follows:

The input and output signals from the process to be studied are measured simultaneously and analyzed by a mathematical model. During the measurement the model parameters (order and matrix coefficients) are updated iteratively by comparing the output from this model with the output from the process. The deviations of these outputs contribute to the convergence of the model.

When finally the evaluated output from model is identical to the measured output - within predefined margins - the process is said to be "identified" and relevant information is stored in the model's matrix coefficients. The model order is then also evaluated and optimized by using Akaike criterion [Ref. 1].

Now this model can be used to study various dynamic characteristics of the process. By disturbing the model we can find step responses, time constants and transfer functions as well as complex cause-consequence relations.

Also testing of sensor conditions (aging) is frequently done using process identification.

6.2 Applications for fusion

At JET some applications have recently been tested in the following areas [Ref. 2]:

- The introduction of Beryllium in the wall changed the mass balance in the plasma. The conventional controller for this reason has been redesigned to bring the system back to acceptable performance. However, with the knowledge of current dynamics (through identification) and expected reference signals a performance beyond what is possible with the previous technology could be achieved. An enhancement in terms of an

adaptive feed-forward solution superimposed on the established system is being considered within JET. Some preliminary attempts of running an identifier on real data has so far given some encouraging results.

- The plasma positioning control in the vertical direction is complicated by the fact that the open loop system is unstable; it has a pole in the right-hand half of the s-plane. This pole is normally moved across to the left-hand side (the stable region) through adequate design of feedback. In this case, however, the position of the pole is not constant, which keeps changing the conditions for the feedback stabilisation. In order to maintain the overall performance of the system the pole position has to be identified and the feedback algorithm updated accordingly. A feasibility study addressing this problem has been carried out by UMIST for NET with participation from JET [2].

- A leakage detection module for the magnet cooling system has been designed and tested. Normal expansion variations due to the operation at JET is several orders of magnitude higher than that relating to leaks in the system. An identifier with the ability to distinguish between expected and unexpected variations was developed within JET.

As concerns NET we propose to study the application of process identification methods to burn control. Within this area a promising approach is

- a survey of relevant diagnostics as input to a system to identify "underlying common" information about the dynamics of the plasma

- to investigate the area of burn control under the aspect of:

- which (set of) diagnostics are suitable candidates for necessary control loops

is there a necessity to improve their performance

- is there a necessity to "develop" new diagnostics

to contribute to the better understanding between the demands and needs from physicists and control experts.

6.3 Present preparative activities

A key experiment has been designed and will be conducted during the first half of 1990. We will make use of process identification technique for an investigation in fusion plasma dynamics.

Software for the solution of a set of model equations for burn dynamics has been developed, c.f. Sec. 2. In situations near marginal stability (weakly stable and weakly unstable) a carefully selected "persistent" excitation will be used, together with noise-corrupted data from the solutions of the evolution equations. Analyzing these data using process identification an attempt will be made to recover a couple of the system parameters, e.g. the energy and particle confinement times. Thus a comparison is possible with the values assumed when generating the data. If this is successful an attempt will be made to identify, in a situation with feedback control, both the intrinsic dynamics of the open system and the control actions taken.

In this way it will be possible to demonstrate the feasibility of using process identification on known systems as concerns burning fusion plasma.

Later, based on this experience, it should be possible to use real data (e.g. from JET) to evaluate interesting dynamical parameters from measured plasma shots in order to study practical contributions to burn control.

6.4 Process identification and physical models

Several different forms and methods for system identification exist. The theoretical approach with a system description in terms of equations derived from basic physical principles represents one extreme case. Such a theory is desirable but it may be incomplete, having flaws and limited validity or involve unknown parameters.

At the other extreme we have a black-box model in which the system is treated based on measured input-output signal relations with a non-physical mathematical formalism, which takes very little credit of "known" relations derived from a physical theory.

It is an interesting fact that between these two cases there exists a whole spectrum of intermediate possibilities in which one can include what is known about the system from physical analyses, e.g. the structure and order of the system. This knowledge can then be used - together with sampled input/output data - to determine unknown parameters. It seems that the "state space" formalism of control theory is particularly well suited for this since the laws of physics are very often formulated in terms of differential equations. This is indeed the case with the present problem of burn control.

In a real situation, even if a theory exists which claims to describe the pertinent phenomena, one may also use a black-box model to check the validity of the theory. This should be of interest for burn control since zero-dimensional systems describing burn with different dimensions exist; a black-box identification model may thus be helpful to distinguish between the theoretical models in a systematic way, still based on an experimental approach.

References

1. Akaike criterion: H. Akaike "A new look at the statistical model identification". IEEE Trans an autom control, Vol. AC-19, No. 6, Dec. 1974.

2. JET-applications, 2.a. Hans Brelen, private communication, 2 b. Working group on plasma positioning: Hans Brelen (JET), Mike Brown, (NET), Peter Wellstedt, (Manchester University, UMIST).

7. Future work

In order to complete this prestudy of burn control issues for NET/ITER some particular issues related to the power balance, actuator techniques and control techniques have to be further investigated. Particularly we intend to study the following:

- The potential of using the P_α-signal as a basis for control purposes extended by a reconstruction of n and T and utilizing state-space control, Sec. 2.5.

- To find an optimized way to chose between several actuators in order to reduce the input effort and undesired side effects, Sec. 2.5.

- Different minimization criteria with respect to desired and actual signal and their implications on the requirements on the actuators in terms of, e.g. maximum power rate, power and energy, Sec. 2.5.

- An extension of 0-D models to allow for a more complete description of radial transport, Sec. 3.7.

- Further development on finding criteria for the time evolution of given initial profiles, Sec. 4.2.

- The complicating effect of sawtooth oscillations for (i) the interpretation of neutron emission data and (ii) the feedback control of a subignited reactor plasma, Sec. 4.3.

- The practical implications for control by variation of effective minor radius will be investigated. If feasible the idea could possibly be supported by a numerical study where the 1-D power balance equation would be solved. Concerning dynamic stabilization, where the preliminary conclusion was that the method is ineffective, the remaining open questions will be studied, Sec. 4.4.

- The burn dynamics by means of process identification. The coupled power equations will be used for generating signals (with some noise added) for a process identification in a numerical experiment to be performed early 1990. The purpose is to study the potential of this technique for conditions of relevance for burn control, Sec. 6.3.

A closer interaction with the NET-team particularly with the purpose of studying the technical aspects of the actuators and diagnostics is also foreseen.

Acknowledgements

This work was performed within a NET Article-6 contract, NET 89-193. Valuable discussions with Drs. K. Borrass and F. Engelmann are gratefully acknowledged. Mrs. B. Larsson managed, with a tremendous effort, to decipher an initially hopeless manuscript for which we thank her. Thanks are also due to Mr. M. Nestorsson, for his help in the preparation of some of the figures.